
# EMVA Standard 1288

## Standard for Characterization of Image Sensors and Cameras

Release 3.1

December 30, 2016

Issued by

European Machine Vision Association

www.emva.org

## Contents

**Acknowledgements**

EMVA 1288 is an initiative driven by the industry and living from the personal initiative of the supporting companies and institutions delegates as well as from the support of these organizations. Thanks to this generosity the presented document can be provided free of charge to the users of this standard. EMVA thanks those contributors (see Appendix E) in the name of the whole vision community.



**About this Standard**

EMVA has started the initiative to define a unified method to measure, compute and present specification parameters and characterization data for cameras and image sensors used for machine vision applications. The standard does not define what nature of data should be disclosed. It is up to the component manufacturer to decide if he wishes to publish typical data, data of an individual component, guaranteed data, or even guaranteed performance over life time of the component. However the component manufacturer shall clearly indicate what the nature of the presented data is.

The standard is organized in different sections, each addressing a group of specification parameters, assuming a certain physical behavior of the sensor or camera under certain boundary conditions. Additional sections covering more parameters and a wider range of sensor and camera products will be added successively. There are *compulsory* sections, of which all measurements must be made and of which all required data and graphics must be included in a datasheet using the EMVA1288 logo. Further there are *optional* sections which may be skipped for a component where the respective data is not relevant or the mathematical model is not applicable. Each datasheet shall clearly indicate which sections of the EMVA1288 standard are enclosed.

It may be necessary for the manufacturer to indicate additional, component specific information, not defined in the standard, to fully describe the performance of image sensor or camera products, or to describe physical behavior not covered by the mathematical models of the standard. It is possible in accordance with the EMVA1288 standard to include such data in the same datasheet. However the data obtained by procedures not described in the current release of the EMVA1288 standard must be clearly designated and grouped in a separate section. It is not permitted to use parameter designations defined in any of the EMVA1288 modules for such additional information not acquired or presented according the EMVA1288 procedures.

The standard is intended to provide a concise definition and clear description of the measurement process and to benefit the Automated Vision Industry by providing fast, comprehensive and consistent access to specification information for cameras and sensors. It will be particularly beneficial for those who wish to compare cameras or who wish to calculate system performance based on the performance specifications of an image sensor or a camera.

# 1 Introduction and Scope

This release of the standard covers monochrome and color digital cameras with linear photo response characteristics. It is valid for area scan and line scan cameras. Analog cameras can be described according to this standard in conjunction with a frame grabber; similarly, image sensors can be described as part of a camera. If not specified otherwise, the term camera is used for all these items.

The standard text is parted into four sections describing the mathematical model and parameters that characterize cameras and sensors with respect to

- Section 2: linearity, sensitivity, and noise for monochrome and color cameras,
- Section 3: dark current,
- Section 4: sensor array nonuniformities and defect pixels characterization,

a section with an overview of the required measuring setup (Section 5), and five sections that detail the requirements for the measuring setup and the evaluation methods for

- Section 6: linearity, sensitivity, and noise,
- Section 7: dark current,
- Section 8: sensor array nonuniformities and defect pixels characterization,
- Section 9: spectral sensitivity,

The detailed setup is not regulated in order not to hinder progress and the ingenuity of the implementers. It is, however, mandatory that the measuring setups meet the properties specified by the standard. Section 10 finally describes how to produce the EMVA 1288 datasheets. Appendix B describes the notation and Appendix C details the changes to release 2.

It is important to note that the standard can only be applied if the camera under test can actually be described by the mathematical model on which the standard is based. If these conditions are not fulfilled, the computed parameters are meaningless with respect to the camera under test and thus the standard cannot be applied. Currently, electron multiplying cameras (EM CCD, [2, 3]) and cameras that are sensitive in the deep ultraviolet, where more than one electron per absorbed photon is generated [7], are not covered by the standard. The general assumptions include

1. The amount of photons collected by a pixel depends on the product of irradiance $E$ (units $\mathrm{W/m^2}$) and exposure time $t_{\mathrm{exp}}$ (units s), i. e., the radiative energy density $Et_{\mathrm{exp}}$ at the sensor plane.
2. The sensor is linear, i. e., the digital signal $y$ increases linearly with the number of photons received.
3. All noise sources are wide-sense stationary and white with respect to time and space. The parameters describing the noise are invariant with respect to time and space.
4. Only the total quantum efficiency is wavelength dependent. The effects caused by light of different wavelengths can be linearly superimposed.
5. Only the dark current is temperature dependent.

These assumptions describe the properties of an *ideal* camera or sensor. A real sensor will depart more or less from an ideal sensor. As long as the deviation is small, the description is still valid and it is one of the tasks of the standard to describe the degree of deviation from an ideal behavior. However, if the deviation is too large, the parameters derived may be too uncertain or may even render meaningless. Then the camera cannot be characterized using this standard. The standard can also not be used for cameras that clearly deviate from one of these assumptions. For example, a camera with a logarithmic instead of a linear response curve cannot be described with the present release of the standard.

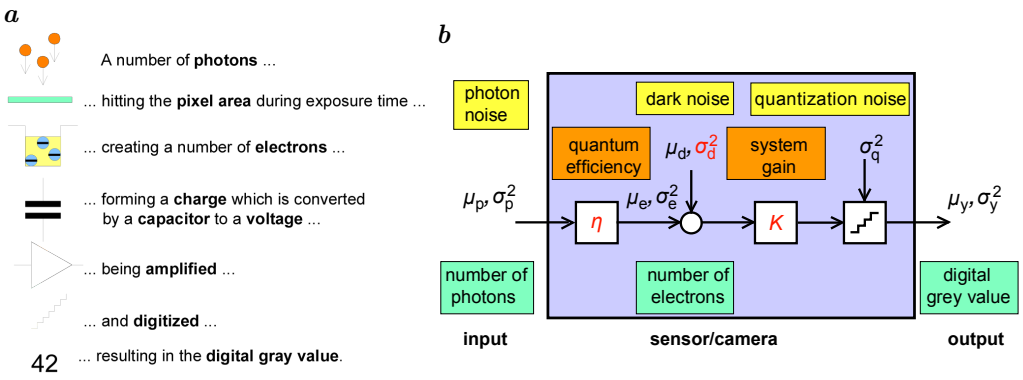


***Figure 1:*** ***a*** *Physical model of the camera and* ***b*** *Mathematical model of a single pixel. Figures separated by comma represent the mean and variance of a quantity; unknown model parameters are marked in red.*

# 2 Sensitivity, Linearity, and Noise

This section describes how to characterize the sensitivity, linearity, and temporal noise of an image sensor or camera [4–6, 9].

## 2.1 Linear Signal Model

As illustrated in Fig. 1, a digital image sensor essentially converts photons hitting the pixel area during the exposure time by a sequence of steps finally into a digital number. During the exposure time on average $\mu_p$ photons hit the whole area $A$ of a single pixel. A fraction

$$\eta(\lambda) = \frac{\mu_e}{\mu_p} \tag{1}$$

of them, the *total quantum efficiency*, is absorbed and accumulates $\mu_e$ charge units.[1] The total quantum efficiency as defined here refers to the total area occupied by a single sensor element (pixel) not only the light sensitive area. Consequently, this definition includes the effects of fill factor and microlenses. As expressed in Eq. (1), the quantum efficiency depends on the wavelength of the photons irradiating the pixel.

The mean number of photons that hit a pixel with the area $A$ during the exposure time $t_{\text{exp}}$ can be computed from the irradiance $E$ on the sensor surface in $\text{W/m}^2$ by

$$\mu_p = \frac{AEt_{\text{exp}}}{h\nu} = \frac{AEt_{\text{exp}}}{hc/\lambda}, \tag{2}$$

using the well-known quantization of the energy of electromagnetic radiation in units of $h\nu$. With the values for the speed of light $c = 2.99792458 \cdot 10^8\,\text{m/s}$ and Planck's constant $h = 6.6260755 \cdot 10^{-34}\,\text{Js}$, the photon irradiance is given by

$$\mu_p[\text{photons}] = 5.034 \cdot 10^{24} \cdot A[\text{m}^2] \cdot t_{\text{exp}}[\text{s}] \cdot \lambda[\text{m}] \cdot E\left[\frac{\text{W}}{\text{m}^2}\right], \tag{3}$$

or in more handy units for image sensors

$$\mu_p[\text{photons}] = 50.34 \cdot A[\mu\text{m}^2] \cdot t_{\text{exp}}[\text{ms}] \cdot \lambda[\mu\text{m}] \cdot E\left[\frac{\mu\text{W}}{\text{cm}^2}\right]. \tag{4}$$

These equations are used to convert the irradiance calibrated by radiometers in units of $\text{W/cm}^2$ into photon fluxes required to characterize imaging sensors.

In the camera electronics, the charge units accumulated by the photo irradiance is converted into a voltage, amplified, and finally converted into a digital signal $y$ by an analog

[1] The actual mechanism is different for CMOS sensors, however, the mathematical model for CMOS is the same as for CCD sensors

digital converter (ADC). The whole process is assumed to be linear and can be described by a single quantity, the *overall system gain* $K$ with units DN/e$^-$, i. e., digits per electrons.[2] Then the mean digital signal $\mu_y$ results in

$$\mu_y = K(\mu_e + \mu_d) \quad \text{or} \quad \mu_y = \mu_{y.\text{dark}} + K\mu_e, \tag{5}$$

where $\mu_d$ is the mean number electrons present without light, which result in the mean dark signal $\mu_{y.\text{dark}} = K\mu_d$ in units DN with zero irradiation. Note that the dark signal will generally depend on other parameters, especially the exposure time and the ambient temperature (Section 3).

With Eqs. (1) and (2), Eq. (5) results in a linear relation between the mean gray value $\mu_y$ and the number of photons irradiated during the exposure time onto the pixel:

$$\boxed{\mu_y = \mu_{y.\text{dark}} + K\eta\,\mu_p = \mu_{y.\text{dark}} + K\eta\frac{\lambda A}{hc}\,E\,t_{\text{exp}}.} \tag{6}$$

This equation can be used to verify the linearity of the sensor by measuring the mean gray value in relation to the mean number of photons incident on the pixel and to measure the *responsivity* $K\eta$ from the slope of the relation. Once the overall system gain $K$ is determined from Eq. (9), it is also possible to estimate the quantum efficiency from the responsivity $K\eta$.

### 2.2 Noise Model

The number of charge units (electrons) fluctuates statistically. According to the laws of quantum mechanics, the probability is Poisson distributed. Therefore the variance of the fluctuations is equal to the mean number of accumulated electrons:

$$\sigma_e^2 = \mu_e. \tag{7}$$

This noise, often referred to as *shot noise* is given by the basic laws of physics and equal for all types of cameras.

All other noise sources depend on the specific construction of the sensor and the camera electronics. Due to the linear signal model (Section 2.1), all noise sources add up. For the purpose of a camera model treating the whole camera electronics as a black box it is sufficient to consider only two additional noise sources. All noise sources related to the sensor read out and amplifier circuits can be described by a signal independent normal-distributed noise source with the variance $\sigma_d^2$. The final analog digital conversion (Fig. 1b) adds another noise source that is uniform-distributed between the quantization intervals and has a variance $\sigma_q^2 = 1/12\,\text{DN}^2$ [9].Because the variances of all noise sources add up linearly, the total temporal variance of the digital signal $y$, $\sigma_y^2$, is given according to the laws of error propagation by

$$\sigma_y^2 = K^2\left(\sigma_d^2 + \sigma_e^2\right) + \sigma_q^2 \tag{8}$$

Using Eqs. (7) and (5), the noise can be related to the measured mean digital signal:

$$\boxed{\sigma_y^2 = \underbrace{K^2\sigma_d^2 + \sigma_q^2}_{\text{offset}} + \underbrace{K}_{\text{slope}}(\mu_y - \mu_{y.\text{dark}}).} \tag{9}$$

This equation is central to the characterization of the sensor. From the linear relation between the variance of the noise $\sigma_y^2$ and the mean photo-induced gray value $\mu_y - \mu_{y.\text{dark}}$ it is possible to determine the overall system gain $K$ from the slope and the dark noise variance $\sigma_d^2$ from the offset. This method is known as the *photon transfer method* [6, 8].

### 2.3 Signal-to-Noise Ratio (SNR)

The quality of the signal is expressed by the signal-to-noise ratio (SNR), which is defined as

$$\text{SNR} = \frac{\mu_y - \mu_{y.\text{dark}}}{\sigma_y}. \tag{10}$$

[2] DN is a dimensionless unit, but for sake of clarity, it is better to denote it specifically.

Using Eqs. (6) and (8), the SNR can then be written as

$$\boxed{\mathrm{SNR}(\mu_p) = \frac{\eta\mu_p}{\sqrt{\sigma_d^2 + \sigma_q^2/K^2 + \eta\mu_p}}.} \tag{11}$$

Except for the small effect caused by the quantization noise, the overall system gain $K$ cancels out so that the SNR depends only on the quantum efficiency $\eta(\lambda)$ and the dark signal noise $\sigma_d$ in units $\mathrm{e}^-$. Two limiting cases are of interest: the high-photon range with $\eta\mu_p \gg \sigma_d^2 + \sigma_q^2/K^2$ and the low-photon range with $\eta\mu_p \ll \sigma_d^2 + \sigma_q^2/K^2$:

$$\mathrm{SNR}(\mu_p) \approx \begin{cases} \sqrt{\eta\mu_p}, & \eta\mu_p \gg \sigma_d^2 + \sigma_q^2/K^2, \\ \dfrac{\eta\mu_p}{\sqrt{\sigma_d^2 + \sigma_q^2/K^2}}, & \eta\mu_p \ll \sigma_d^2 + \sigma_q^2/K^2. \end{cases} \tag{12}$$

This means that the slope of the SNR curve changes from a linear increase at low irradiation to a slower square root increase at high irradiation.

A real sensor can always be compared to an *ideal* sensor with a quantum efficiency $\eta = 1$, no dark noise ($\sigma_d = 0$) and negligible quantization noise ($\sigma_q/K = 0$). The SNR of an ideal sensor is given by

$$\mathrm{SNR}_{\mathrm{ideal}} = \sqrt{\mu_p}. \tag{13}$$

Using this curve in SNR graphs, it becomes immediately visible how close a real sensor comes to an ideal sensor.

### 2.4 Signal Saturation and Absolute Sensitivity Threshold

For an $k$-bit digital camera, the digital gray values are in a range between the 0 and $2^k - 1$. The practically useable gray value range is smaller, however. The mean dark gray value $\mu_{y.\mathrm{dark}}$ must be higher than zero so that no significant underflow occurs by temporal noise and the dark signal nonuniformity (for an exact definition see Section 6.5). Likewise the maximal usable gray value is lower than $2^k - 1$ because of the temporal noise and the photo response nonuniformity.

Therefore, the *saturation irradiation* $\mu_{p.\mathrm{sat}}$ is defined as the maximum of the measured relation between the variance of the gray value and the irradiation in units photons/pixel. The rational behind this definition is that according to Eq. (9) the variance is increasing with the gray value but is decreasing again, when the digital values are clipped to the maximum digital gray value $2^k - 1$.

From the saturation irradiation $\mu_{p.\mathrm{sat}}$ the *saturation capacity* $\mu_{e.\mathrm{sat}}$ can be computed:

$$\boxed{\mu_{e.\mathrm{sat}} = \eta\mu_{p.\mathrm{sat}}.} \tag{14}$$

The saturation capacity must not be confused with the *full-well capacity*. It is normally lower than the full-well capacity, because the signal is clipped to the maximum digital value $2^k - 1$ before the physical saturation of the pixel is reached.

The *minimum detectable irradiation* or *absolute sensitivity threshold*, $\mu_{p.\mathrm{min}}$ can be defined by using the SNR. It is the mean number of photons required so that the SNR is equal to 1.

For this purpose, it is required to know the inverse function to Eq. (11), i. e., the number of photons required to reach a given SNR. Inverting Eq. (11) results in

$$\boxed{\mu_p(\mathrm{SNR}) = \frac{\mathrm{SNR}^2}{2\eta}\left(1 + \sqrt{1 + \frac{4(\sigma_d^2 + \sigma_q^2/K^2)}{\mathrm{SNR}^2}}\right).} \tag{15}$$

In the limit of large and small SNR, this equation approximates to

$$\mu_p(\mathrm{SNR}) \approx \begin{cases} \dfrac{\mathrm{SNR}^2}{\eta}\left(1 + \dfrac{\sigma_d^2 + \sigma_q^2/K^2}{\mathrm{SNR}^2}\right), & \mathrm{SNR}^2 \gg \sigma_d^2 + \sigma_q^2/K^2, \\ \dfrac{\mathrm{SNR}}{\eta}\left(\sqrt{\sigma_d^2 + \sigma_q^2/K^2} + \dfrac{\mathrm{SNR}}{2}\right), & \mathrm{SNR}^2 \ll \sigma_d^2 + \sigma_q^2/K^2. \end{cases} \tag{16}$$

This means that for almost all cameras, i. e., when $\sigma_d^2+\sigma_q^2/K^2 \gg 1$, the absolute sensitivity threshold can be well approximates by

$$\mu_p(\mathrm{SNR}=1)=\mu_{p.\min} \approx \frac{1}{\eta}\left(\sqrt{\sigma_d^2+\sigma_q^2/K^2}+\frac{1}{2}\right)=\frac{1}{\eta}\left(\frac{\sigma_{y.\mathrm{dark}}}{K}+\frac{1}{2}\right). \tag{17}$$

The ratio of the signal saturation to the absolute sensitivity threshold is defined as the *dynamic range* (DR):

$$\mathrm{DR}=\frac{\mu_{p.\mathrm{sat}}}{\mu_{p.\min}}. \tag{18}$$

# 3 Dark Current

## 3.1 Mean and Variance

The dark signal $\mu_d$ introduced in the previous section, see Eq. (5), is not constant. The main reason for the dark signal are thermally induced electrons. Therefore, the dark signal should increase linearly with the exposure time

$$\mu_d=\mu_{d.0}+\mu_{\mathrm{therm}}=\mu_{d.0}+\mu_I t_{\mathrm{exp}}. \tag{19}$$

In this equation all quantities are expressed in units of electrons ($\mathrm{e}^-$/pixel). These values can be obtained by dividing the measured values in the units DN by the overall system gain $K$ (Eq. (9)).

The quantity $\mu_I$ is named the *dark current*, given in the units $\mathrm{e}^-$/(pixel s). According to the laws of error propagation, the variance of the dark signal is then given as

$$\sigma_d^2=\sigma_{d.0}^2+\sigma_{\mathrm{therm}}^2=\sigma_{d.0}^2+\mu_I t_{\mathrm{exp}}, \tag{20}$$

because the thermally induced electrons are Poisson distributed as are the light induced ones in Eq. (7) with $\sigma_{\mathrm{therm}}^2=\mu_{\mathrm{therm}}$. If a camera or sensor has a dark current compensation the dark current can only be characterized using Eq. (20).

## 3.2 Temperature Dependence

The temperature dependence of the dark current is modeled in a simplified form. Because of the thermal generation of charge units, the dark current increases roughly exponentially with the temperature [5, 7, 13]. This can be expressed by

$$\mu_I=\mu_{I.\mathrm{ref}}\cdot 2^{(T-T_{\mathrm{ref}})/T_d}. \tag{21}$$

The constant $T_d$ has units K or $^o$C and indicates the temperature interval that causes a doubling of the dark current. The temperature $T_{\mathrm{ref}}$ is a reference temperature at which all other EMVA 1288 measurements are performed and $\mu_{I.\mathrm{ref}}$ the dark current at the reference temperature. The measurement of the temperature dependency of the dark current is the only measurement to be performed at different ambient temperatures, because it is the only camera parameter with a *strong* temperature dependence.

# 4 Spatial Nonuniformity and Defect Pixels

The model discussed so far considered only a single pixel. All parameters of an array of pixels, will however vary from pixel to pixel. Sometimes these nonuniformities are called *fixed pattern noise*, or *FPN*. This expression is however misleading, because inhomogeneities are no noise, which makes the signal varying in time. The inhomogeneity may only be distributed randomly. Therefore it is better to name this effect *nonuniformity*.

Essentially there are two basic nonuniformities. First, the dark signal can vary from pixel to pixel. This effect is called *dark signal nonuniformity*, abbreviated by *DSNU*. Second, the variation of the sensitivity is called *photo response nonuniformity*, abbreviated by *PRNU*.

The EMVA 1288 standard describes nonuniformities in three different ways. The spatial variance (Section 4.1) is a simply overall measure of the spatial nonuniformity. The spectrogram method (Section 4.2) offers a way to analyze patterns or periodic spatial variations,

which may be disturbing to image processing operations or the human observer. Finally, the characterization of defect pixels (Section 4.3) is a flexible method to specify unusable or defect pixels according to application specific criteria.

### 4.1 Spatial Variances, DSNU, and PRNU

For all types of spatial nonuniformities, spatial variances can be defined. This results in equations that are equivalent to the temporal noise but with another meaning. The averaging is performed over all pixels of a sensor array. The mean of the mean of a sequence of $L$ $M \times N$ dark and the 50% saturation images, $\langle \boldsymbol{y}_{\text{dark}} \rangle$ and $\langle \boldsymbol{y}_{50} \rangle$, are given by:

$$\mu_{y.\text{dark}} = \frac{1}{MN} \sum_{m=0}^{M-1} \sum_{n=0}^{N-1} \langle y_{\text{dark}} \rangle [m][n], \quad \mu_{y.50} = \frac{1}{MN} \sum_{m=0}^{M-1} \sum_{n=0}^{N-1} \langle y_{50} \rangle [m][n], \tag{22}$$

where $M$ and $N$ are the number of rows and columns of the image and $m$ and $n$ the row and column indices of the array, respectively. Likewise, the *spatial variances* $s^2$ of dark and 50% saturation images are given by:

$$s^2_{y.\text{dark}} = \frac{1}{MN-1} \sum_{m=0}^{M-1} \sum_{n=0}^{N-1} (\langle y_{\text{dark}} \rangle [m][n] - \mu_{y.\text{dark}})^2, \tag{23}$$

$$s^2_{y.50} = \frac{1}{MN-1} \sum_{m=0}^{M-1} \sum_{n=0}^{N-1} (\langle y_{50} \rangle [m][n] - \mu_{y.50})^2. \tag{24}$$

All spatial variances are denoted with the symbol $s^2$ to distinguish them easily from the temporal variances $\sigma^2$.

The DSNU and PRNU values of the EMVA 1288 standard are based on spatial standard deviations:

$$\begin{aligned} \text{DSNU}_{1288} &= s_{y.\text{dark}}/K \qquad \text{(units e}^-\text{)}, \\ \text{PRNU}_{1288} &= \frac{\sqrt{s^2_{y.50} - s^2_{y.\text{dark}}}}{\mu_{y.50} - \mu_{y.\text{dark}}} \quad \text{(units \%)}. \end{aligned} \tag{25}$$

The index 1288 has been added to these definitions because many different definitions of these quantities can be found in the literature. The $\text{DSNU}_{1288}$ is expressed in units $\text{e}^-$; by multiplying with the overall system gain $K$ it can also be given in units DN. The $\text{PRNU}_{1288}$ is defined as a standard deviation relative to the mean value. In this way, the $\text{PRNU}_{1288}$ gives the spatial standard deviation of the photoresponse nonuniformity in % from the mean.

### 4.2 Types of Nonuniformities

The variances defined in the previous sections give only an over-all measure of the spatial nonuniformity. It can, however, not be assumed in general that the spatial variations are normally distributed. This would only be the case if the spatial variations are totally random, i. e., that there are no spatial correlation of the variations. However, for an adequate description of the spatial nonuniformities several effects must be considered:

**Gradual variations.** Manufacturing imperfections can cause gradual low-frequency variations over the whole chip. This effect is not easy to measure because it requires a very homogeneous irradiation of the chip, which is difficult to achieve. Fortunately this effect does not really degrade the image quality significantly. A human observer does not detect it at all and additional gradual variations are introduced by lenses (shading, vignetting) and nonuniform illumination. Therefore, gradual variations must be corrected with the complete image system anyway for applications that demand a flat response over the whole sensor array.

**Periodic variations.** This type of distortion is caused by electronic interferences in the camera electronic and is very nasty, because the human eye detects such distortions very sensitively. Likewise many image processing operations are disturbed. Therefore it is important to detect this type of spatial variation. This can most easily be done

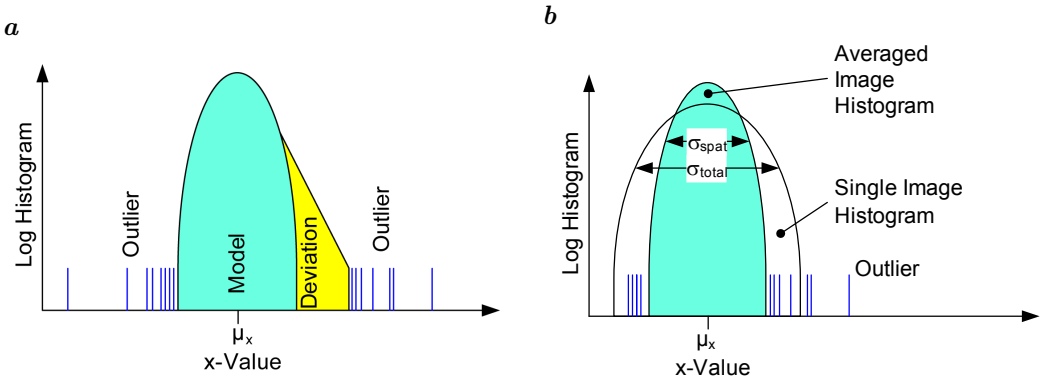


***Figure 2:*** *Logarithmic histogram of spatial variations* ***a*** *Showing comparison of data to model and identification of deviations from the model and of outliers,* ***b*** *Comparison of logarithmic histograms from single images and averaged over many images.*

by computing a spectrogram, i. e., a power spectrum of the spatial variations. In the spectrogram, periodic variations show up as sharp peaks with specific spatial frequencies in units cycles/pixel.

**Outliers.** This are single pixels or cluster of pixels that show a significantly deviation from the mean. This type of nonuniformity is discussed in detail in Section 4.3.

**Random variations.** If the spatial nonuniformity is purely random, i. e., shows no spatial correlation, the power spectrum is flat, i. e., the variations are distributed equally over all wave numbers. Such a spectrum is called a *white spectrum*.

From this description it is obvious that the computation of the spectrogram, i. e., the power spectrum, is a good tool.

### 4.3 Defect Pixels

As application requirements differ, it will not be possible to find a common denominator to exactly define when a pixel is defective and when it is not. Therefore it is more appropriate to provide *statistical information* about pixel properties in the form of histograms. In this way anybody can specify how many pixels are unusable or defect using application-specific criteria.

**4.3.1 Logarithmic Histograms.** It is useful to plot the histograms with logarithmic y-axis for two reasons (Fig. 2a). Firstly, it is easy to compare the measured histograms with a normal distribution, which shows up as a negatively shaped parabola in a logarithmic plot. Thus it is easy to see deviations from normal distributions. Secondly, also rare outliers, i. e., a few pixels out of millions of pixels can be seen easily.

All histograms have to be computed from pixel values that come from averaging over many images. In this way the histograms only reflect the statistics of the spatial noise and the temporal noise is averaged out. The statistics from a single image is different. It contains the total noise, i.e. the spatial and the temporal noise. It is, however, useful to see in how far the outliers of the averaged image histogram will vanish in the temporal noise (Fig. 2b).

It is hard to generally predict in how far a deviation from the model will impact the final applications. Some of them will have human spectators, while others use a variety of algorithms to make use of the images. While a human spectator is usually able to work well with pictures in which some pixel show odd behaviors, some algorithms may suffer from it. Some applications will require defect-free images, some will tolerate some outliers, while other still have problems with a large number of pixels slightly deviating. All this information can be read out of the logarithmic histograms.

**4.3.2 Accumulated Histograms.** A second type of histograms, accumulated histogram is useful in addition (Fig. 3). It is computed to determine the ratio of pixels deviating by more than a certain amount. This can easily be connected to the application requirements.

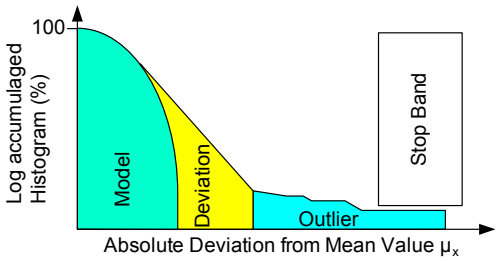


***Figure 3:*** *Accumulated histogram with logarithmic y-axis.*

Quality criteria from camera or chip manufacturers can easily be drawn in this graph. Usually the criteria is, that only a certain amount of pixels deviates more than a certain threshold. This can be reflected by a rectangular area in the graph. Here it is called *stop band* in analogy to drawings from high-frequency technologies that should be very familiar to electronics engineers.

### 4.4 Highpass Filtering

This section addresses the problem that the photoresponse distribution may be dominated by gradual variations in illumination source, especially the typical fall-off of the irradiance towards the edges of the sensor. Low-frequency spatial variations of the image sensor, however, are of less importance, because of two reasons. Firstly, lenses introduce a fall-off towards the edges of an image (*lens shading*). Except for special low-shading lenses, this effect makes a significant contribution to the low-frequency spatial variations. Secondly, almost all image processing operations are not sensitive to gradual irradiation changes. (See also discussion in Section 4.2 under item gradual variations.)

In order to show the properties of the camera rather than the properties of an imperfect illumination system, a highpass filtering is applied before computing the histograms for defect pixel characterization discussed in Sections 4.3.1–4.3.2. In this way the effect of low spatial frequency sensor properties is suppressed. The highpass filtering is performed using a box filter, for details see Appendix C.5.

***Table 1:*** *List of all EMVA 1288 measurements with classification into mandatory and optional measurements.*

| Type of measurement | Mandatory | Reference |
|---|---|---|
| Sensitivity, temporal noise and linearity | Y | Section 6 |
| Nonuniformity | Y | Sections 8.1 and 8.2 |
| Defect pixel characterization | Y | Section 8.4 |
| Dark current | Y | Section 7.1 |
| Temperature dependence on dark current | N | Section 7.2 |
| Spectral measurements $\eta(\lambda)$ | N | Section 9 |

# 5 Overview Measurement Setup and Methods

The characterization according to the EMVA 1288 standard requires three different measuring setups:

1. A setup for the measurement of sensitivity, linearity and nonuniformity using a homogeneous monochromatic light source (Sections 6 and 8).
2. The measurement of the temperature dependency of the dark current requires some means to control the temperature of the camera. The measurement of the dark current at the standard temperature requires no special setup (Section 7).
3. A setup for spectral measurements of the quantum efficiency over the whole range of wavelength to which the sensor is sensitive (Section 9).

Each of the following sections describes the measuring setup and details the measuring procedures. All camera settings (besides the variation of exposure time where stated) *must be identical* for all measurements. For different settings (e. g., gain) different sets of measurements must be acquired and different sets of parameters, containing all parameters which may influence the characteristic of the camera, must be presented. Line-scan sensors are treated as if they were area-scan sensors. Acquire at least 100 lines into one image and then proceed as with area-scan cameras for all evaluations except for the computation of vertical spectrograms (Section 8.2).

Not all measurements are mandatory as summarized in Table 1. A data sheet is only EMVA 1288 compliant if the results of *all* mandatory measurements from at least one camera are reported. If optional measurements are reported, these measurements must fully comply to the corresponding EMVA 1288 procedures.

All example evaluations shown in Figs. 5–14 come from simulated data — and thus served also to verify the methods and algorithms. A 12-bit $640 \times 480$ camera was simulated with a quantum efficiency $\eta = 0.5$, a dark value of 29.4 DN, a gain $K = 0.1$, a dark noise $\sigma_0 = 30\,\mathrm{e}^-$ ($\sigma_{y.\mathrm{dark}} = 3.0$ DN), and with a slightly nonlinear camera characteristics. The DSNU has a white spatial standard deviation $s_w = 1.5$ DN and two sinusoidal patterns with an amplitude of 1.5 DN and frequencies in horizontal and vertical direction of 0.04 and 0.2 cylces/pixel, respectively. The PRNU has a white spatial standard deviation of 0.5%. In addition, a slightly inhomogenous illumination with a quadratic fall-off towards the edges by about 3% was simulated.

# 6 Methods for Sensitivity, Linearity, and Noise

## 6.1 Geometry of Homogeneous Light Source

For the measurement of the sensitivity, linearity and nonuniformity, a setup with a light source is required that irradiates the image sensor homogeneously without a mounted lens. Thus the sensor is illuminated by a diffuse disk-shaped light source with a diameter $D$ placed in front of the camera (Fig. 4a) at a distance $d$ from the sensor plane. Each pixel must receive light from the whole disk under a angle. This can be defined by the *f-number*

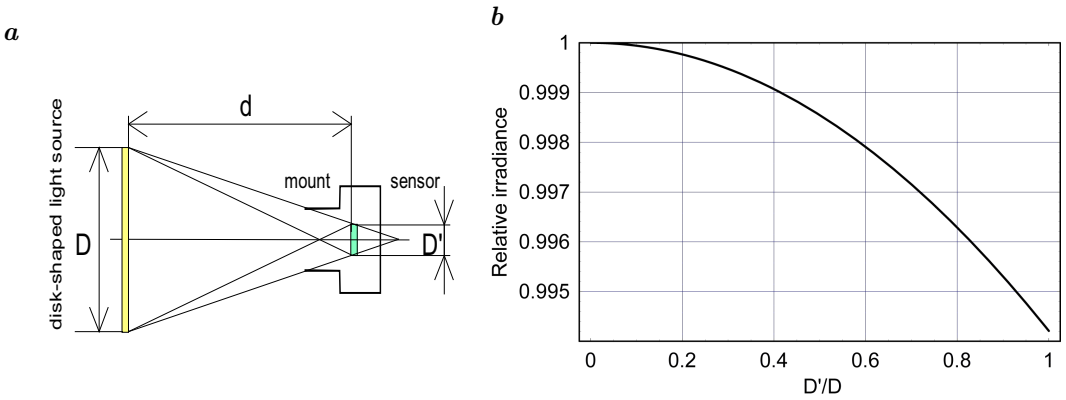


***Figure 4:*** ***a*** *Optical setup for the irradiation of the image sensor by a disk-shaped light source,* ***b*** *Relative irradiance at the edge of a image sensor with a diameter $D'$, illuminated by a perfect integrating sphere with an opening $D$ at a distance $d = 8D$.*

of the setup, which is is defined as:

$$f_\# = \frac{d}{D}. \tag{26}$$

Measurements performed according to the standard require an $f$-number of 8.

The best available homogeneous light source is an integrating sphere. Therefore it is not required but recommended to use such a light source. But even with a perfect integrating sphere, the homogeneity of the irradiation over the sensor area depends on the diameter of the sensor, $D'$, as shown in Fig. 4b [10, 11]. For a distance $d = 8 \cdot D$ (f-number 8) and a diameter $D'$ of the image sensor equal to the diameter of the light source, the decrease is only about 0.5% (Fig. 4b). Therefore the diameter of the sensor area should not be larger than the diameter of the opening of the light source.

A real illumination setup even with an integrating sphere has a much worse inhomogeneity, due to one or more of the following reasons:

**Reflections at lens mount.** Reflections at the walls of the lens mount can cause significant inhomogeneities, especially if the inner walls of the lens mount are not suitably designed and are not carefully blackened and if the image sensor diameter is close to the free inner diameter of the lens mount.

**Anisotropic light source.** Depending on the design, a real integrating sphere will show some residual inhomogeneities. This is even more the case for other types of light sources.

Therefore it is essential to specify the spatial nonuniformity of the illumination, $\Delta E$. It should be given as the difference between the maximum and minimum irradiation over the area of the measured image sensor divided by the average irradiation in percent:

$$\Delta E[\%] = \frac{E_{\max} - E_{\min}}{\mu_E} \cdot 100. \tag{27}$$

It is recommended that $\Delta E$ is not larger than 3%. This recommendation results from the fact that the linearity should be measured over a range from 5–95% of the full range of the sensor (see Section 6.7).

## 6.2 Spectral Properties of Light Source

Measurements of *gray-scale cameras* are performed with monochromatic light with a *full width half maximum* (FWHM) of less than 50 nm. For monochrome cameras it is recommended to use a light source with a center wavelength to the maximum quantum efficiency of the camera under test. For the measurement of *color cameras*, the light source must be operated with different wavelength ranges, each wavelength range must be close to the maximum response of one of the corresponding color channels. Normally these are the colors blue, green, and red, but it could be any combination of color channels including channels in the ultraviolet and infrared.

Such light sources can be achieved, e. g., by a light emitting diode (LED) or a broadband light source such as incandescent lamp or an arc lamp with an appropriate bandpass filter. The peak wavelength $\lambda_p$, the centroid wavelength $\lambda_c$, and the full width half maximum (FWHM) of the light source must be specified. The best approach is to measure these quantities directly using a spectrometer. It is also valid to use the specifications given from the manufacturer of the light source. For a halogen light source with a bandpass filter, a good estimate of the spectral distribution of the light source is given by multiplying the corresponding blackbody curve with the transmission curve of the filter.

Use the centroid wavelength of the light source for computation of the number of photons according to Eq. (2).

### 6.3 Variation of Irradiation

Basically, there are three possibilities to vary the irradiation of the sensor, i. e., the radiation energy per area received by the image sensor:

**I. Constant illumination with variable exposure time.**
With this method, the light source is operated with constant radiance and the irradiation is changed by the variation of the exposure time. The irradiation $H$ is given as the irradiance $E$ times the exposure time $t_{\text{exp}}$ of the camera. Because the dark signal generally may depend on the exposure time, it is required to measure the dark image at *every* exposure time used. The absolute calibration depends on the true exposure time being equal to the exposure time set in the camera.

**II. Variable continuous illumination with constant exposure time.**
With this method, the radiance of the light source is varied by any technically possible way that is sufficiently reproducible. With LEDs this is simply achieved by changing the current. The irradiation $H$ is given as the irradiance $E$ times the exposure time $t_{\text{exp}}$ of the camera. Therefore the absolute calibration depends on the true exposure time being equal to the exposure time set in the camera.

**III. Pulsed illumination with constant exposure time.**
With this method, the irradiation of the sensor is varied by the pulse length of the LED. When switched on, a constant current is applied to the LEDs. The irradiation $H$ is given as the LED irradiance $E$ times the pulse length $t$. The sensor exposure time is set to a constant value, which is larger than the maximum pulse length for the LEDs. The LEDs pulses are triggered by the "integrate enable" or "strobe out" signal from the camera. The LED pulse must have a short delay to the start of the integration time and it must be made sure that the pulse fits into the exposure interval so that there are no problems with trigger jittering. The pulsed illumination technique must not be used with rolling shutter mode. Alternatively it is possible to use an external trigger source in order to trigger the sensor exposure and the LED flashes synchronously.

According to the basic assumption number one and two made in Section 1, all three methods are equivalent because the amount of photons collected and thus the digital gray value depends only on the product of the irradiance E and the time, the radiation is applied. Therefore all three measurements are equivalent for a camera that adheres to the linear signal model as described in Section 2.1. Depending on the available equipment and the properties of the camera to be measured, one of the three techniques for irradiation variation can be chosen.

### 6.4 Calibration of Irradiation

The irradiation must be calibrated absolutely by using a calibrated photodiode put at the place of the image sensor. The calibration accuracy of the photodiode as given by the calibration agency plus possible additional errors related to the measuring setup must be specified together with the data. The accuracy of absolute calibrations are typically between 3% and 5%, depending on the wavelength of the light. The reference photodiode should be recalibrated at least every second year. This will then also be the *minimum systematic error* of the measured quantum efficiency.

The precision of the calibration of the different irradiance levels must be much more higher than the absolute accuracy in order to apply the photon transfer method (Sections 2.2 and 6.6) and to measure the linearity (Sections 2.1 and 6.7) of the sensor with sufficient accuracy. Therefore, the standard deviation of the calibration curve from a linear regression must be lower than 0.1% of the maximum value.

### 6.5 Measurement Conditions for Linearity and Sensitivity

**Temperature.** The measurements are performed at room temperature or a controlled temperature elevated above the room temperature. The type of temperature control must be specified. Measure the temperature of the camera housing by placing a temperature sensor at the lens mount with good thermal contact. If a cooled camera is used, specify the set temperature. Do not start measurements before the camera has come into thermal equilibrium.

**Digital resolution.** Set the number of bits as high as possible in order to minimize the effects of quantization on the measurements.

**Gain.** Set the gain of the camera as small as possible without saturating the signal due to the full well capacity of any pixel (this almost never happens). If with this minimal gain, the dark noise $\sigma_{y.\mathrm{dark}}$ is smaller than 0.5 DN, the dark noise cannot be measured reliably. (This happens only in the rare case of a 8-bit camera with a high-quality sensor.) Then only an upper limit for the temporal dark noise can be calculated. The dynamic range is then limited by the quantization noise.

**Offset.** Set the offset of the camera as small as possible but large enough to ensure that the dark signal including the temporal noise and spatial nonuniformity does not cause any significant underflow. This can be achieved by setting the offset at a digital value so that less than about 0.5% of the pixels underflow, i. e., have the value zero. This limit can easily be checked by computing a histogram and ensures that not more than 0.5% of the pixels are in the bin zero.

**Distribution of irradiance values.** Use at least 50 equally spaced exposure times or irradiation values resulting in digital gray value from the dark gray value and the maximum digital gray value. Only for production measurements as few as 9 suitably chosen values can be taken.

**Number of measurements taken.** Capture two images at each irradiation level. To avoid transient phenomena when the live grab is started, images A and B are taken from a live image series. It is also required to capture two images each without irradiation (dark images) at *each* exposure time used for a proper determination of the mean and variance of the dark gray value, which may depend on the exposure time (Section 3).

### 6.6 Evaluation of the Measurements according to the Photon Transfer Method

As described in section Section 2, the application of the photon transfer method and the computation of the quantum efficiency requires the measurement of the mean gray values and the temporal variance of the gray together with the irradiance per pixel in units photons/pixel. The mean and variance are computed in the following way:

**Mean gray value.** The mean of the gray values $\mu_y$ over *all* $N$ pixels in the active area at each irradiation level is computed from the two captured $M \times N$ images $y^A$ and $y^B$ as

$$\mu_y = \frac{1}{2NM} \sum_{m=0}^{M-1} \sum_{n=0}^{N-1} (y^A[m][n] + y^B[m][n]) \tag{28}$$

averaging over all rows $i$ and columns $j$. In the same way, the mean gray value of dark images, $\mu_{y.\mathrm{dark}}$, is computed.

**Temporal variance of gray value.** Normally, the computation of the temporal variance would require the capture of many images. However on the assumptions put forward in Section 1, the noise is stationary and homogenous, so that it is sufficient to take the

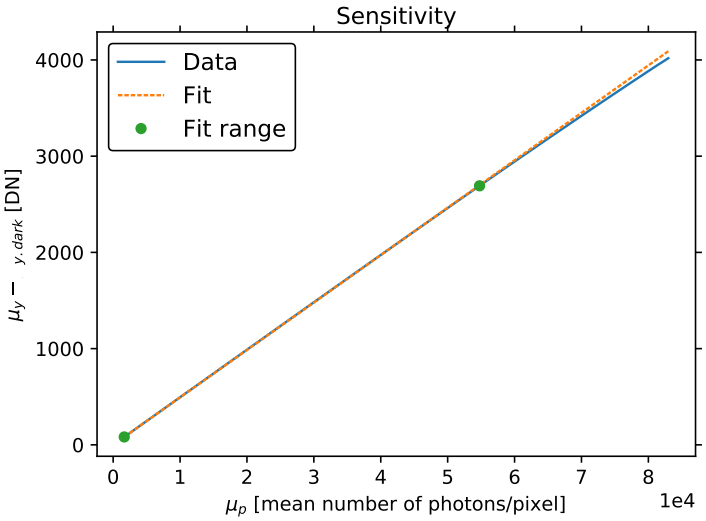


***Figure 5:*** *Example of a measuring curve to determine the responsivity $R = K\eta$ of a camera. The graph draws the measured mean photo-induced gray values $\mu_y - \mu_{y.dark}$ versus the irradiation $H$ in units photons/pixel and the linear regression line used to determine $R = K\eta$. The red dots marks the 0 – 70% range of saturation that is used for the linear regression. For color cameras, the graph must contain these items for each color channel. If the irradiation is changed by changing the exposure time (method I in Section 6.3), a second graph must be provided which shows $\mu_{y.dark}$ as a function of the exposure time $t_{exp}$.*

mean of the squared difference of the two images

$$\sigma_y^2 = \frac{1}{2NM} \sum_{m=0}^{M-1} \sum_{n=0}^{N-1} (y^A[m][n] - y^B[m][n])^2. \tag{29}$$

Because the variance of the difference of two values is the sum of the variances of the two values, the variance computed in this way must be divided by two as indicated in Eq. (29).

The estimation of derived quantities according to the photon transfer method is performed as follows:

**Saturation.** The saturation gray value $\mu_{y.\mathrm{sat}}$ is given as the mean gray value where the variance $\sigma_y$ has a maximum value (see green square in Fig. 6). To find this value the following procedure is recommended: The saturation point is given by scanning the photon transfer curve from the right and given by the first point where the next two points are lower. For a smooth photon transfer curve this is equivalent to taking the absolute maximum. Any other deterministic algorithm may be used. This algorithm must be documented and must give identical results to those from the published reference data sets available via the EMVA website `www.emva.org`.

**Responsivity $R$.** According to Eq. (6), the slope of the relation

$$\mu_y - \mu_{y.\mathrm{dark}} = R\mu_p$$

(with zero offset) gives the responsivity $R = K\eta$. For this regression all data points must be used in the range between the minimum value and 70% saturation ($0.7 \cdot (\mu_{y.\mathrm{sat}} - \mu_{y.\mathrm{dark}})$) (Fig. 5).

**Overall system gain $K$.** According to Eq. (9), the slope of the relation

$$\sigma_y^2 - \sigma_{y.\mathrm{dark}}^2 = K(\mu_y - \mu_{y.\mathrm{dark}})$$

(with zero offset) gives the absolute gain factor $K$. Select the same range of data points as for the estimation of the responsivity (see above, and Fig. 6).

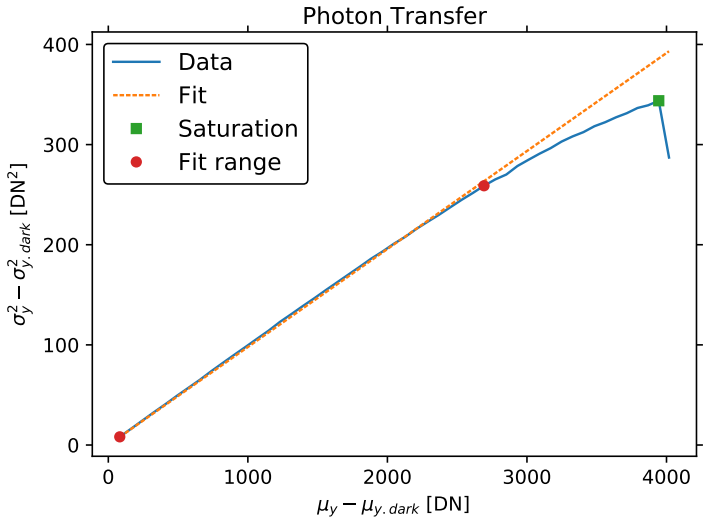


***Figure 6:*** *Example of a measuring curve to determine the overall system gain $K$ of a camera (photo transfer curve). The graph draws the measured photo-induced variance $\sigma_y^2 - \sigma_{y.dark}^2$ versus the mean photo-induced gray values $\mu_y - \mu_{y.dark}$ and the linear regression line used to determine the overall system gain $K$. The green dots mark the 0 – 70% range of saturation that is used for the linear regression. The system gain $K$ is given with its one-sigma statistical uncertainty in percent, computed from the linear regression.*

Compute a least-squares linear regression of $\sigma_y^2 - \sigma_{y.\mathrm{dark}}^2$ versus $\mu_y - \mu_{y.\mathrm{dark}}$ over the selected range and specify the gain factor $K$.

**Quantum efficiency $\eta$.** The quantum efficiency $\eta$ is given as the ratio of the responsivity $R = K\eta$ and the overall system gain $K$:

$$\eta = \frac{R}{K}. \tag{30}$$

For monochrome cameras, the quantum efficiency is thus obtained only for a single wavelength band with a bandwidth no wider than 50 nm. Because all measurements for color cameras are performed for all color channels, quantum efficiencies for all theses wavelengths bands are obtained and to be reported. For color camera systems that use a color filter pattern any pixel position in the repeated pattern should be analyzed separately. For a Bayer pattern, for example, there are four color channels in total, mostly two separate green channels, a blue channel, and a red channel.

**Temporal dark noise.** It is required to compute two values.

1. For measurement method I with variable exposure time in Section 6.3 the temporal dark noise is found as the offset of the linear correspondence of the $\sigma_{y.\mathrm{dark}}^2$ over the exposure times. For the measurement method II and III in Section 6.3 make an extra measurement at a minimal exposure time to estimate $\sigma_{y.\mathrm{dark}}$. Use this value to compute the dynamic range. This value gives the actual performance of the camera at the given bit resolution and thus includes the quantization noise.
2. In order to compute the temporal dark noise in units $\mathrm{e}^-$ (a quantity of the sensor *without* the effects of quantization), subtract quantization noise and use

$$\sigma_d = \sqrt{(\sigma_{y.\mathrm{dark}}^2 - \sigma_q^2)} \Big/ K. \tag{31}$$

If $\sigma_{y.\mathrm{dark}}^2 < 0.24$, the temporal noise is dominated by the quantization noise and no reliable estimate is possible (Section C.4). Then $\sigma_{y.\mathrm{dark}}$ must be set to 0.49 and the upper limit of the temporal dark noise in units $\mathrm{e}^-$ *without* the effects of quantization is given by

$$\sigma_d < \frac{0.40}{K}. \tag{32}$$

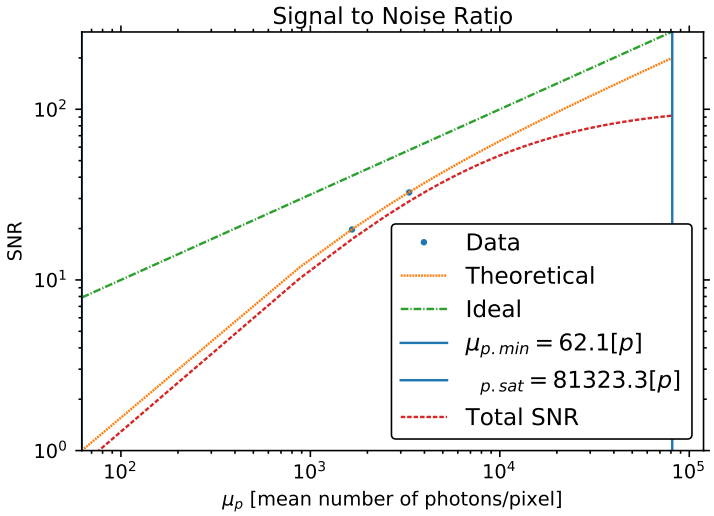


***Figure 7:*** *Example of a SNR graph. It contains the measured SNR values, the theoretical curve according to the linear camera model Eq. (11) determined with the measured $\sigma_d^2$ and $\eta$ values, the theoretical curve according to Eq. (48) including in addition the effect of spatial nonuniformities (DSNU and PRNU), and the SNR curve for an ideal sensor Eq. (13) with no dark and quantization noise and a quantum efficiency $\eta$ of 1. The absolute sensitivity threshold and the saturation capacity are marked by vertical dashed lines.*

**Absolute sensitivity threshold $\mu_{p.\mathbf{min}}$.** Use definition Eq. (17) in Section 2.4 to compute the absolute sensitivity threshold $\mu_{p.\min}$.

**Saturation capacity $\mu_{p.\mathbf{sat}}$.** Calculate the saturation capacity $\mu_{p.\mathrm{sat}}$ as number of photons which corresponds to the maximum of the measured relation between the variance of the gray value and the photons. The saturation capacity $\mu_{e.\mathrm{sat}}$ in $e^-$ is given by Eq. (14).

**Signal-to-noise ratio (SNR).** The measured mean and the variance of the gray values are used to compute the SNR according to Eq. (10). These values are plotted in a double logarithmic plot together with the theoretical curve for the linear model after Eq. (11) using the measured quantum efficiency $\eta$ and the temporal dark noise $\sigma_d$ and the quantization noise (Fig. 7). Also compute the maximum achievable $\mathrm{SNR}_{\max}$ for the saturation irradiation using

$$\mathrm{SNR}_{\max} = \sqrt{\mu_{e.\mathrm{sat}}} \tag{33}$$

and express this value as a ratio, in dB ($20 \log_{10}$ SNR), and in bits ($\log_2$ SNR).

**Dynamic range (DR).** Use the definition Eq. (18) in Section 2.4 to compute the dynamic range. It should be given as a ratio, in dB ($20 \log_{10}$ DR), and in bits ($\log_2$ DR).

### 6.7 Evaluation of Linearity

According to Section 6.5 at least 9 pairs of mean digital gray $\mu_y[i]$ and irradiation values $H[i]$ are available. The linearity is determined by computing a least-squares linear regression minimizing the *relative* deviation in the digital gray value axis from the linear relation

$$y = a_0 + a_1 H \tag{34}$$

with an offset $a_0$ and a slope $a_1$ (Fig. 8a). In the following equations the abbreviation $y[i] = \mu_y[i] - \mu_{\mathrm{y.dark}}[i]$ is used.[3] Because *relative* deviations are minimized, not

$$\sum_i [y[i] - (a_0 + a_1 H[i])]^2$$

[3]The index $i$ in $\mu_{\mathrm{y.dark}}[i]$) applies only for method I to vary the irradiation (see Section 6.3). For methods II and III it is a single mean dark value $\mu_{\mathrm{y.dark}}$.

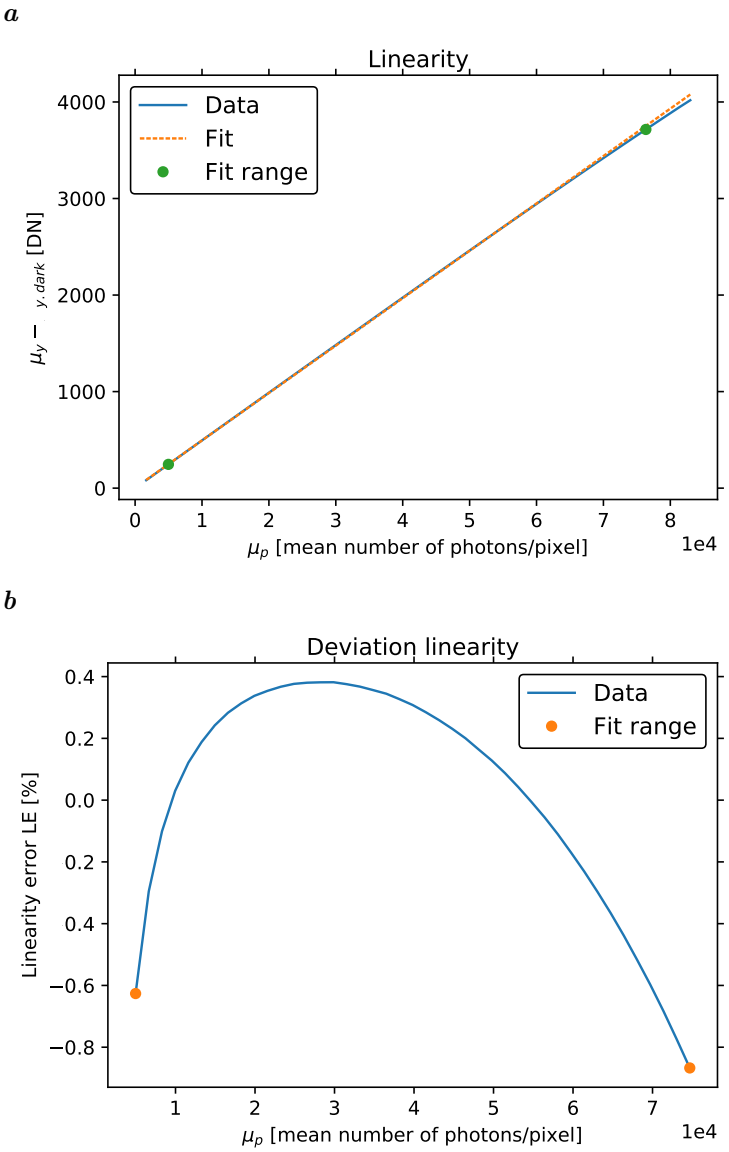


***Figure 8:*** *Example for the evaluation of the linearity:* ***a*** *Mean gray value minus the dark value versus the irradiation plus the linear regression curve covering* all *measured values. The dots mark the 5 – 95% range of saturation that is used for the linearity regression.* ***b*** *Percentage of the deviation from the linear regression to determine the linearity error LE. The 5% and 95% saturation values are marked by dots, which range from* $\min(\delta_y)$ *to* $\max(\delta_y)$*, see Eqs. (38) and (39).*

is minimized but

$$\sum_i \frac{1}{y[i]^2} \left[ y[i] - (a_0 + a_1 H[i]) \right]^2 .$$

This is equivalent to a weighted least squares regression, where each data point $y[i]$ gets the weight $1/y[i]^2$. The resulting equations for estimating the offset $a_0$ and the slope $a_1$ are

$$a_0 = \frac{1}{\Delta} \left[ \sum H[i]/y[i] \sum H[i]/y[i]^2 - \sum H[i]^2/y[i]^2 \sum 1/y[i] \right] \tag{35}$$

and

$$a_1 = \frac{1}{\Delta} \left[ \sum H[i]/y[i]^2 \sum 1/y[i] - \sum H[i]/y[i] \sum 1/y[i]^2 \right] \tag{36}$$

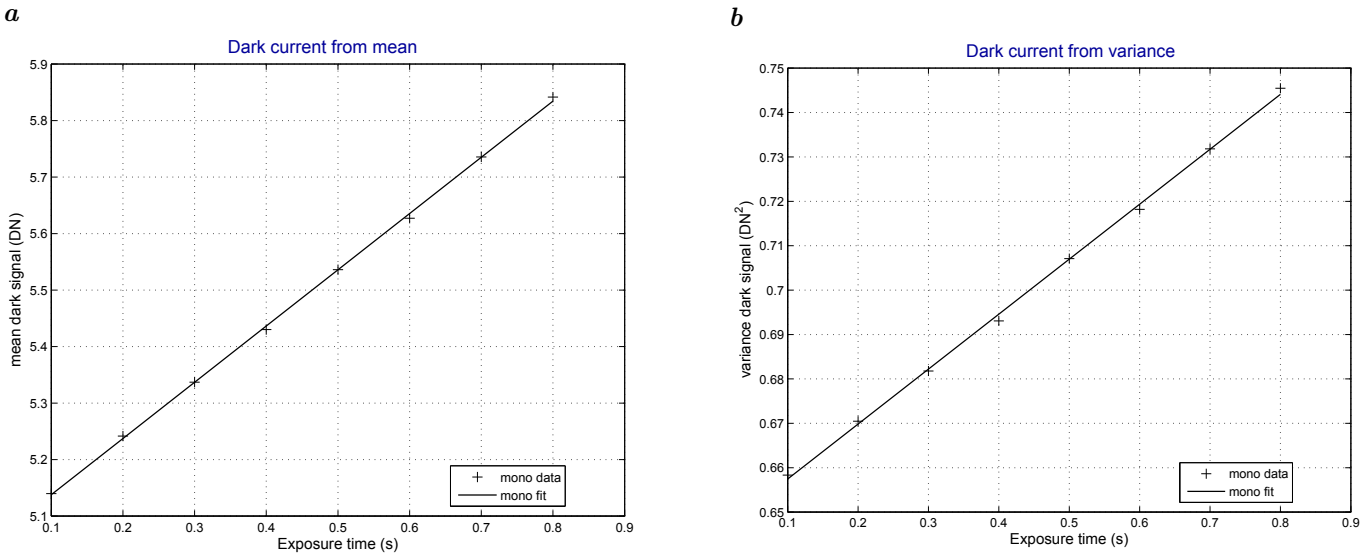


***Figure 9:*** *Examples for dark current measurements: plot of the* ***a*** *dark value versus the exposure time. The linear regressions line are also shown.*

with

$$\Delta = \left(\sum H[i]/y[i]^2\right)^2 - \sum H[i]^2/y[i]^2 \sum 1/y[i]^2 \tag{37}$$

using the math for linear least squares regression [1, 12]. All sums in this section are computed with data values $y[i], H[i]$ in the range between 5% and 95% of the saturation capacity $\mu_{\text{y.sat}} - \mu_{\text{y.dark}}$.

Using this regression, the relative deviation from the regression can be computed by

$$\delta_y[i]\ [\%] = 100\,\frac{y[i] - (a_0 + a_1 H[i])}{a_0 + a_1 H[i]}. \tag{38}$$

The linearity error is then defined as the maximal deviation and the minimal deviation in the range between 5% and 95% of the saturation capacity.

$$\text{LE}_{\max} = \max(\delta_y), \quad \text{and} \quad \text{LE}_{\min} = \min(\delta_y), \tag{39}$$

and thus defines the maxima of the positive and negative deviation from the linear regression.

# 7 Methods for Dark Current

## 7.1 Evaluation of Dark Current at One Temperature

Dark current measurements require no illumination source. From Eqs. (19) and (20) in Section 3 it is evident that the dark current can either be measured from the linear increase of the mean or the variance of the dark gray value $y_{\text{dark}}$ with the exposure time. The preferred method is, of course, the measurement of the mean, because the mean can be estimated more accurately than the variance. If, however, the camera features a dark current compensation, the dark current must be estimated using the variance.

At least six equally spaced exposure times must be chosen. For low dark currents, it might be required to choose much longer exposure times than for the sensitivity, linearity, and noise measurements.

The dark current is then given as the slope in the relation between the exposure time and mean and/or variance of the dark value (Fig. 9). A linear least squares regression of the measured dark values gives the dark current in units DN/s. Use the measured gain $K$ (units DN/e$^-$) to express the dark current also in units e$^-$/s.

If the camera's exposure time is not set long enough to result in meaningful values for the dark current, this value still must be reported together with its one-sigma error from the

regression. In this way at least an upper limit of the dark current can be given, provided that $\mu_I + \sigma_I > 0$. The lower limit of the auto saturation time is then

$$t_{\text{sat}} > \frac{\mu_{e.\text{sat}}}{\mu_I + \sigma_I}. \tag{40}$$

### 7.2 Evaluation of Dark Current with Temperatures

The doubling temperature of the dark current is determined by measuring the dark current as described above for different housing temperatures. The temperatures must vary over the whole range of the operating temperature of the camera. Put a capped camera in a climate exposure cabinet or control its temperature in another suitable way and drive the housing temperature to the desired value for the next measurement. For cameras with internal temperature regulation and cooling of the image sensor no climate cabinet is required. Then the temperature dependence of the dark current can only be measured in the temperature range that can be set.

After a temperature change wait until the camera values are stable. This is most easily done by continuosly measuring the dark values at the largest exposure time. For each temperature, determine the dark current by taking a series of measurements with varying exposure times as described in Section 7.1.

In order to determine the doubling temperature, the logarithm of the dark current must be plotted as a function of the temperature $T$. Then according to Eq. (21), a linear relation is obtained

$$\log_{10} \mu_I = \log_{10} \mu_{I.\text{ref}} + \log_{10} 2 \cdot \frac{T - T_{\text{ref}}}{T_d} \tag{41}$$

and the doubling temperature $T_d$ is given as the inverse slope $a_1$ of a least-squares linear regression as $\log_{10} 2/a_1$.

## 8 Methods for Spatial Nonuniformity and Defect Pixels

The measurements for spatial nonuniformity and the characterization of defect pixels are performed with the same setup as the sensitivity, linearity, and noise, described in Section 6. Therefore, the basics measuring conditions are also the same (Section 6.5).

All quantities describing nonuniformities must be computed from mean gray values averaged over many images. This is because the variance of the temporal noise ($\sigma_y \approx 1\%$) is typically larger than the variance of the spatial variations ($s_y \approx 0.3 - 0.5\%$). The temporal noise can be suppressed by averaging over $L$ images.

The typical figures imply that at least a sequence of $L = 16$ images $\boldsymbol{y}$ are required so that $s_y^2$ becomes large compared to $\sigma_y^2/L$. This low value was chosen so that the method can also be applied for fast inline inspection. However, it is better to suppress the temporal noise to such an extend that it no longer influences the standard deviation of the spatial noise. This requires typically the averaging of $L = 100$–$400$ images:

$$\langle \boldsymbol{y} \rangle = \frac{1}{L} \sum_{l=0}^{L-1} \boldsymbol{y}[l]. \tag{42}$$

This procedure has to be applied to a sequence of dark images and a sequence of images at 50% saturation, resulting in $\langle \boldsymbol{y}_{\text{dark}} \rangle$ and $\langle \boldsymbol{y}_{50} \rangle$, respectively.

### 8.1 Spatial Standard Deviation, DSNU, PRNU and total SNR

The measured variances $s^2_{y.\text{measured}}$ when averaging $L$ images according to Eqs. (23) and (24) have to be corrected for the residual variance of the temporal noise. This is simply done by subtracting the residual temporal variance:

$$s_y^2 = s^2_{y.\text{measured}} - \sigma^2_{y.stack}/L. \tag{43}$$

The variance of the temporal noise must be computed directly from the same stack of images $\boldsymbol{y}[l]$ as the mean of the variance at every pixel using

$$\sigma^2_{s[m][n]} = \frac{1}{L-1}\sum_{l=0}^{L-1}\left(y[l][m][n] - \frac{1}{L}\sum_{l=0}^{L-1}y[l][m][n]\right)^2 \quad \text{and} \quad \sigma^2_{y.\text{stack}} = \frac{1}{NM}\sum_{i=0}^{N-1}\sum_{j=0}^{M-1}\sigma^2_{s[m][n]}. \tag{44}$$

The $\text{DSNU}_{1288}$ and $\text{PRNU}_{1288}$ values are then given according to Eq. (25) in Section 4.1 to

$$\text{DSNU}_{1288} = s_{y.\text{dark}}/K \qquad (\text{units e}^-) \tag{45}$$

and

$$\text{PRNU}_{1288} = \frac{\sqrt{s^2_{y.50} - s^2_{y.\text{dark}}}}{\mu_{y.50} - \mu_{y.\text{dark}}} \qquad (\text{units } \%). \tag{46}$$

The $\text{DSNU}_{1288}$ and $\text{PRNU}_{1288}$ values can be used to include the spatial nonuniformites into the SNR resulting in the total SNR. From the definition of the $\text{PRNU}_{1288}$ in Eq. (46), the variance $s^2_y$ can be expressed as

$$s^2_y = s^2_{y.\text{dark}} + (\text{PRNU}_{1288})^2\,(\mu_y - \mu_{y.\text{dark}})^2$$

With the definition of $\text{DSNU}_{1288}$ in Eq. (45) and substituting the mean values by the mean number of photons using the sensitivity curve Eq. (6) the variance of the spatial inhomogeneity in units $\text{DN}^2$ is given by

$$s^2_y = K^2\text{DSNU}^2_{1288} + \text{PRNU}^2_{1288}K^2\,(\eta\mu_p)^2\,. \tag{47}$$

The variance term $s^2_y/K^2$ (units $\text{e}^-$) due to the spatial nonuniformity can be added to the SNR to yield the total SNR:

$$\boxed{\text{SNR}(\mu_p) = \frac{\eta\mu_p}{\sqrt{\sigma^2_d + \text{DSNU}^2_{1288} + \sigma^2_q/K^2 + \eta\mu_p + \text{PRNU}^2_{1288}\,(\eta\mu_p)^2}}.} \tag{48}$$

This model curve of the total SNR has to be added to the SNR plot in Fig. 7.

### 8.2 Horizontal and Vertical Spectrograms

Spectrograms are computed from the DSNU image $\langle\boldsymbol{y}_{\text{dark}}\rangle$ and the PRNU image $\langle\boldsymbol{y}_{50}\rangle - \langle\boldsymbol{y}_{\text{dark}}\rangle$. Computation of a spectrogram from the 50% saturation image $\langle\boldsymbol{y}_{50}\rangle$ is optional. The computation of the horizontal spectrograms requires the following computing steps:

1. Subtract the mean value from the image $\boldsymbol{y}$.
2. Compute the Fourier transform of each row vector $\boldsymbol{y}[m]$:

$$\hat{y}[m][v] = \frac{1}{\sqrt{N}}\sum_{n=0}^{N-1}y[m][n]\,\exp\left(-\frac{2\pi\text{i}nv}{N}\right) \quad \text{for} \quad 0 \le v < N.. \tag{49}$$

3. Compute the mean power spectrum $p[v]$ averaged over all $M$ row spectra:

$$p[v] = \frac{1}{M}\sum_{m=0}^{M}\hat{y}[m][v]\hat{y}^*[m][v], \tag{50}$$

where the superscript $*$ denotes the complex conjugate. The power spectrum according to Eq. (50) is scaled in such a way that white noise gets a flat spectrum with a mean value corresponding to the spatial variance $s^2_y$.

In the spectrograms the square root of the power spectrum, $\sqrt{p[v]}$, is displayed as a function of the spatial frequency $v/N$ (in units of cycles per pixel) up to $v = N/2$

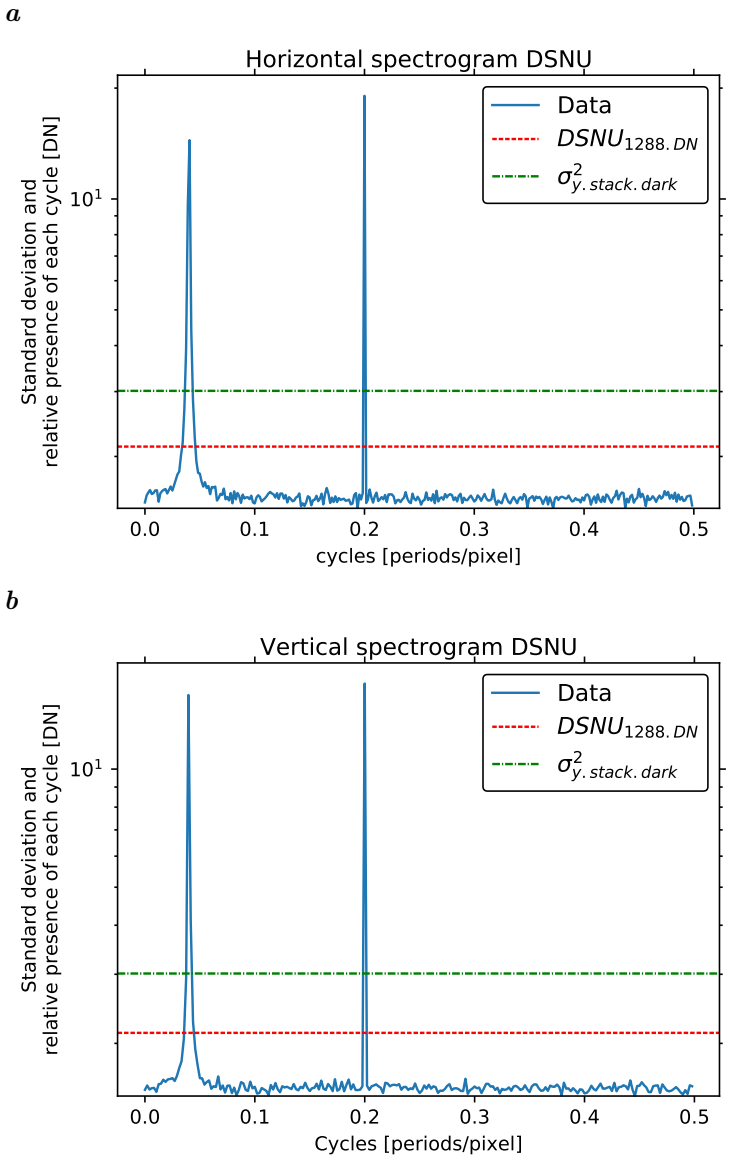


***Figure 10:*** *Example for spectrograms of the dark image:* ***a*** *horizontal spectrogram* ***b*** *vertical spectrogram.*

(Nyquist frequency). It is sufficient to draw only the first part of the power spectrum because the power spectrum has an even symmetry

$$p[N-v] = p[v] \quad \forall v \in [1, N/2].$$

In these plots the level of the white noise corresponds directly to the standard deviation of the spatial white noise. Please note that the peak height in the spectrograms are not equal to the amplitude of corresponding periodic patterns. The amplitude $a$ of a periodic pattern can be computed by adding up the spatial frequencies in the power spectrum belonging to a peak:

$$a = 2\left(\frac{1}{N}\sum_{v_{\min}}^{v_{\max}} p[v]\right)^{1/2}. \tag{51}$$

For the vertical spectrograms (area cameras only), the same computations are performed (Fig. 10b and Fig. 11b). Only rows and columns must be interchanged.

4. Add a line with the $\text{DSNU}_{1288}$ Eq. (45) and $\text{PRNU}_{1288}$ in Eq. (46) to the corresponding spectrogram plots (Figs. 10 and 11). Because the PRNU is given as a relative value to

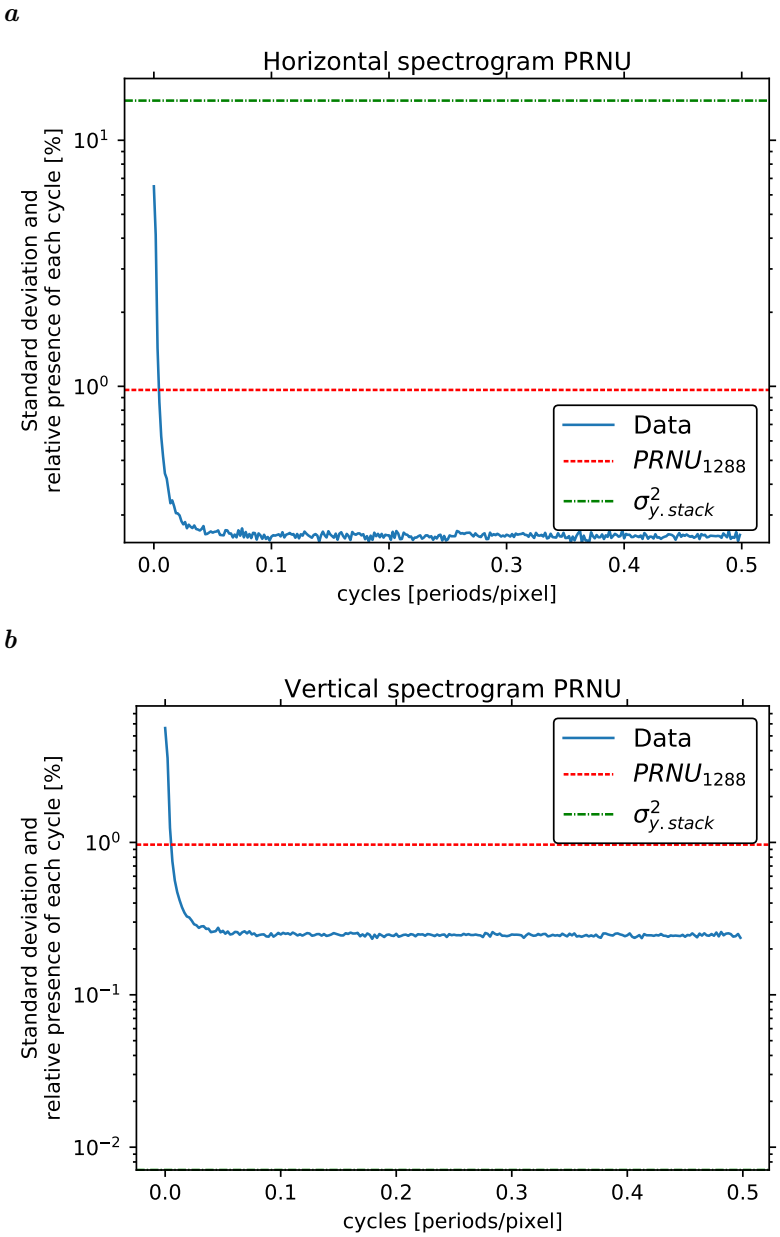


***Figure 11:*** *Example for spectrograms of the photoresponse:* ***a*** *horizontal spectrogram* ***b*** *vertical spectrogram.*

the mean value (Eq. (46)), also the spectrogram values and the temporal noise (see next item) must be divided by the mean values.

5. Also add a line with the standard deviation of the temporal noise, $\sigma_{y.\text{stack}}$ according to Eq. (44) (Figs. 10 and 11). In this way, it is easy to compare spatial and temporal noise.
6. The white noise part of the spatial variance, $s^2_{y.\text{white}}$, is then given by the *median* of the power spectrum. The median value can easily be computed by sorting the $N$ values in the vector $\boldsymbol{p}$ is ascending order to give a new vector $\boldsymbol{p}_{\text{sorted}}$. The median is then the value at the position, $p_{\text{sorted}}[N/2]$.

### 8.3 Horizontal and Vertical Profiles

The spatial nonuniformities are further illustrated by plots of horizontal and vertical profiles of the DSNU and PRNU — in total four plots. Each plot contains four profiles (Example Fig. 12)

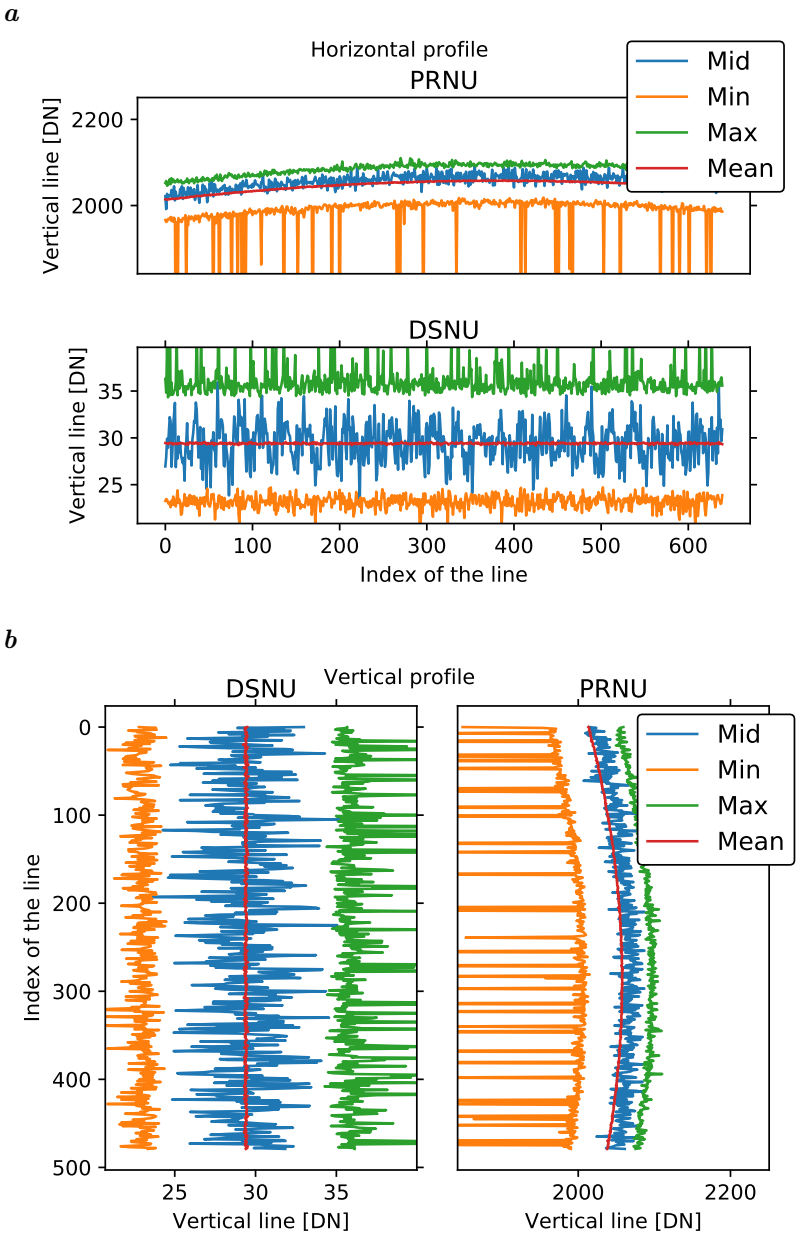


***Figure 12:*** *Example for profile images:* ***a*** *horizontal profiles* ***b*** *vertical profiles.*

**middle:** Horizontal row $M/2$ (vertical profile of column $N/2$) through the center of the image. The correct row/column number is given by integer arithmetics, i. e., the largest integer smaller than the half value; indices start with 0.

**mean:** Average of all rows (all columns).

**max:** Maximum of all rows (all columns) at each horizontal (vertical) position. These profiles nicely show even only few pixels with positive outliers, e. g. hot pixels in the DSNU image.

**min:** Minimum of all rows (all columns) at each horizontal (vertical) position. These profiles nicely show even only few pixels with negative outliers, e. g. less sensitive pixels in the PRNU image.

The profiles are directly computed from the averaged dark image $\langle \boldsymbol{y}_{\text{dark}} \rangle$ and the PRNU image $\langle \boldsymbol{y}_{50} \rangle - \langle \boldsymbol{y}_{\text{dark}} \rangle$ defined in Section 4.1 without applying any corrections such as high-pass filtering.

The ranges of the profiles are set as follows:

**DSNU profiles** Take 0.9 times average of minimum line as lower limit and 1.1 times of average of maximum line as upper limit,

**PRNU profiles** Take 0.9 times average of mean value as lower limit and 1.1 times of average of mean value as upper limit.

Label axes of both DRNU and PRNU profiles with units DN.

### 8.4 Defect Pixel Characterization

Before evaluation of the PRNU image $\langle \boldsymbol{y}_{50} \rangle - \langle \boldsymbol{y}_{\text{dark}} \rangle$, this image must be highpass-filtered as detailed in Section 4.4 and Appendix C.5. No highpass-filtering is performed with the DSNU image $\langle \boldsymbol{y}_{\text{dark}} \rangle$.

The computation of the logarithmic histogram involves the following computing steps for every averaged and highpass-filtered nonuniformity image $\boldsymbol{y}$. The following procedure is suggested to obtain optimally smooth histograms. It is based on the simple fact that nonuniformity images are averaged over $L$ integer-valued images. Therefore they there values are integer multiples of $1/L$ and the optimum interval width is therefore also an integer multiple of $L$.

1. Compute minimum and maximum values $y_{\min}$ and $y_{\max}$ of the image $\boldsymbol{y}$.
2. Part the interval between $y_{\min}$ and $y_{\max}$ into $Q = L(y_{\max} - y_{\min})/I + 1$ bins of equal width with the optimal bin width of $I/L$. Choose an appropriate $(I = 1, 2, 3, \ldots)$ so that the number of bins is lower than or equal to 256. This condition is met by
$$I = \text{floor}\left[\frac{L(y_{\max} - y_{\min})}{256}\right] + 1. \tag{52}$$
3. Compute a histogram with all values of the image using these bins. The bin $q$ to be incremented for a value $y$ is
$$q = \text{floor}\left[\frac{L(y - y_{\min})}{I}\right]. \tag{53}$$
In this way the $Q$ bins of the histogram (indices from 0 to $Q-1$) cover values from $y_{\min}$ to $y_{\max} + (I-1)/L$
The values of the center of the bins as a deviation from the mean value are given as:
$$y[q] = y_{\min} + \frac{I-1}{2L} + q\frac{I}{L}. \tag{54}$$
4. Draw the histogram in a semilogarithmic plot. Use a $x$-axis with the values of the bins relative to the mean value. The $y$ axis must start below 1 so that single outlying pixels can be observed.
5. Add the normal probability density distribution corresponding to the non-white variance $s_{nw}^2$ as a dashed line to the graph obtained for an $M \times N$ image with an interval width $I/L$:
$$p_{\text{normal}}[q] = \frac{I}{L} \cdot \frac{NM}{\sqrt{2\pi}\, s_{nw}} \cdot \exp\left(-\frac{y[q]^2}{2s_{nw}^2}\right). \tag{55}$$

The accumulated logarithmic histogram gives the probability distribution (integral of the probability density function) of the absolute deviation from the mean value. Thus the accumulated logarithmic histogram gives the number of pixels that show at least a certain absolute deviation from the mean in relation to the absolute deviation. The computation involves the following steps:

1. Subtract the mean from the nonuniformity image $\boldsymbol{y}$ and take the absolute value:
$$\boldsymbol{y}' = |\boldsymbol{y} - \mu_y| \tag{56}$$
2. Compute the maximum value $y'_{\max}$ of $\boldsymbol{y}'$; the minimum is zero. The rest of the computations is equivalent to the computation of the non-accumulated histograms of above if $y_{\min}$ is replaced by zero and $y_{\max}$ by $y'_{\max}$.

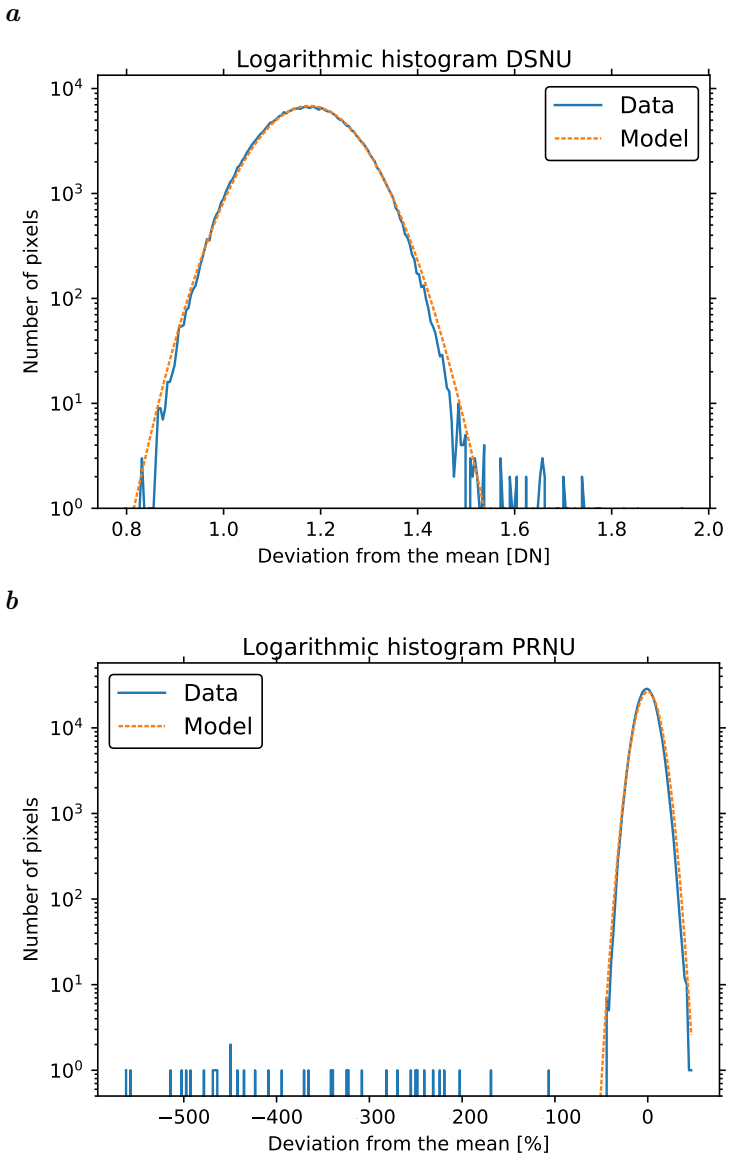


***Figure 13:*** *Example for logarithmic histograms for* **a** *dark signal nonuniformity (DSNU),* **b** *photoresponse nonuniformity (PRNU). The dashed line is the model normal probability density distribution with the non-white standard deviation $s_{nw}$ according to Eq. (55).*

3. Part the interval between 0 and $y'_{\max}$ into $Q = L\,y'_{\max}/I + 1$ bins of equal width with the optimal bin width of $I/L$. Choose an appropriate $(I = 1, 2, 3, \ldots)$ so that the number of bins is lower than or equal to 256. This condition is met by

$$I = \text{floor}\left[\frac{L\,y'_{\max}}{256}\right] + 1. \tag{57}$$

4. Compute a histogram with all values of the image using these bins. The bin $q$ to be incremented for a value $y$ is

$$q = \text{floor}\left(Ly'/I\right). \tag{58}$$

   The values of the center of the bins as a deviation from the mean value are given as:

$$y'[q] = \frac{I-1}{2L} + q\frac{I}{L}. \tag{59}$$

5. Accumulate the histogram. If $h[q']$ are the Q values of the histogram, then the values of

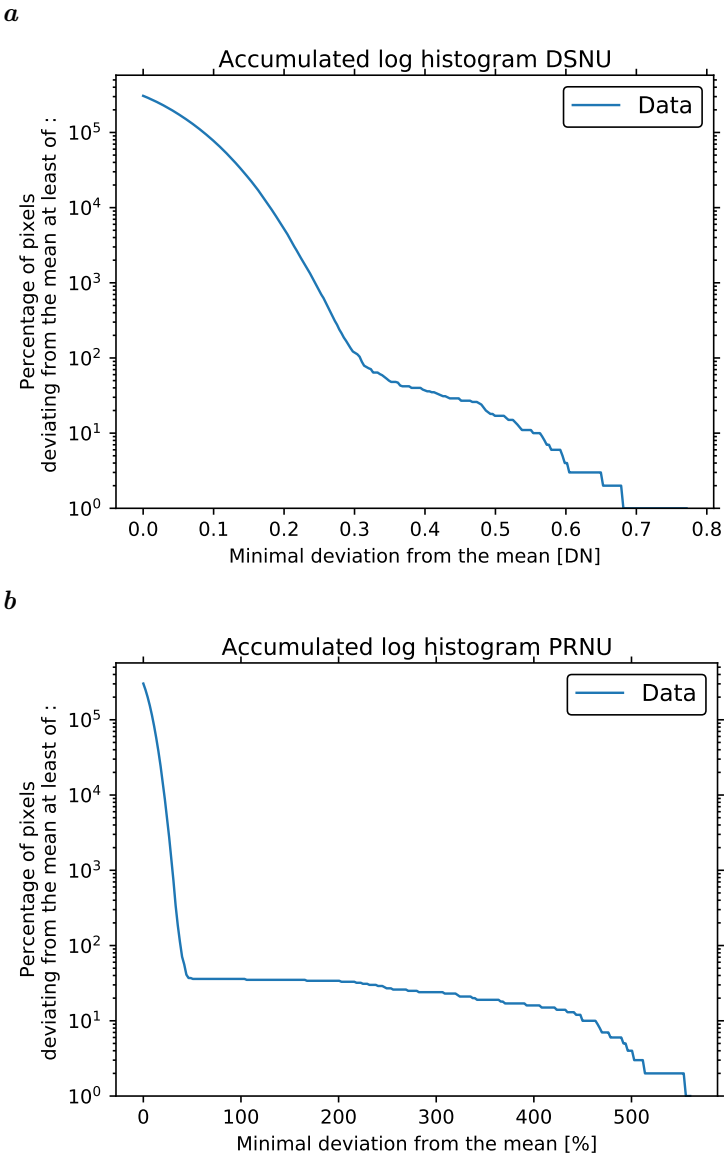


***Figure 14:*** *Example for accumulated logarithmic histograms for* **a** *dark signal nonuniformity (DSNU),* **b** *photoresponse nonuniformity (PRNU).*

the accumulated histogram $H[q]$ are:

$$H[q] = \sum_{q'=q}^{Q} h[q']. \tag{60}$$

6. Draw the accumulated histogram $H[q]$ as a function of $y'[q]$ in a semilogarithmic plot. Use a $x$-axis with the values of the bins relative to the mean value. The $y$ axis must start below 1 so that single outlying pixels can be observed.

Logarithmic histograms and accumulated logarithmic histograms are computed and drawn for both the DSNU and the PRNU. This gives four graphs in total as shown in Figs. 13 and 14.

# 9 Methods for Spectral Sensitivity

## 9.1 Spectral Light Source Setup

The measurement of the spectral dependence of the quantum efficiency requires a separate experimentasl setup with a light source that can be scanned over a certain wavelength range. This apparatus includes either a monochromator with a broadband light source or a light source that can be switched between different wavelengths by any other means. Use an appropriate optical setup to ensure that the light source has the same geometrical properties as detailed in Section 6.1. This means that a light source with a diameter $D$ must evenly illuminate the sensor array or calibration photodiode placed at a distance $d = 8D$ with a diameter $D' \leq D$. A different aperture $d/D$ can be used and must be reported. It is advantageous to set up the whole system in such a way that the photon irradiance is about the same for all wavelengths.

Spectroscopic measurements are quite demanding. It might not be possible to irradiate the whole sensor evenly. Therefore only a section of the sensor may be used for the spectroscopic measurements.

## 9.2 Measuring Conditions

This section summarizes the measuring conditions.

**Sensor area.** Specify the fraction of the sensor area used (all, half, ...).

**Operation point.** The operation point must be the same as for all other measurements.

**Bandwidth.** The FWHM (full width at half maximum) bandwidth of the light source shall be less than 10 nm. If it is technically not feasible to work with such narrow FWHM, the FWHM bandwidth can be enlarged to values up to 50 nm. The FWHM used for the measurement must be reported. Please not that if you use a FWHM larger than 10 nm it will not be possible to evaluate the color rendition of a color sensor, e. g., according to the ISO 13655 and CIE 15.2. Some image sensors show significant oscillations in the quantum efficiency as a function of the wavelength of the light (Fig. 15). If such oscillations occur, the peak positions vary from sensor to sensor. Therefore it is allowed to smooth, provided that the filter procedure is described including the width of the filter.

**Wavelength range.** The scanned wavelength range should cover all wavelength to which the sensor responds. Normally, this includes a wavelength range from at least 350 nm to 1100 nm. For UV sensitive sensors the wavelength range must be extended to correspondingly shorter wavelengths, typically down to 200 nm. If technically feasible, the number of measuring points must be chosen in such a way that the whole wavelength range is covered without gaps. This implies that the distance between neighboring wavelengths is smaller than or equal to the 2 FWHM.

**Signal range.** An exposure time should be set to a value so that sufficiently large signals are obtained for all wavelengths. If the irradiation of the light source shows large variations for different wavelengths, this could require more than one spectral scan with different exposure times. Before and after each wavelength sweep and for every exposure time used, a dark image must be taken.

## 9.3 Calibration

The experimental setup is calibrated in the same way as the monochromatic setup (Section 6.4). The image sensor is replaced by a calibrated photodiode for these measurements. From the measured irradiance at the sensor surface, the number of photons $\mu_p(\lambda)$ collected during the exposure time are computed using Eq. (2).

## 9.4 Evaluation

The measured wavelength dependent quantum efficiency is averaged over all pixels of the sensor or the selected sensor area. For color cameras, the spectral response must be evaluated for all colors separately just in the same way as described at the end of Section 6.6.

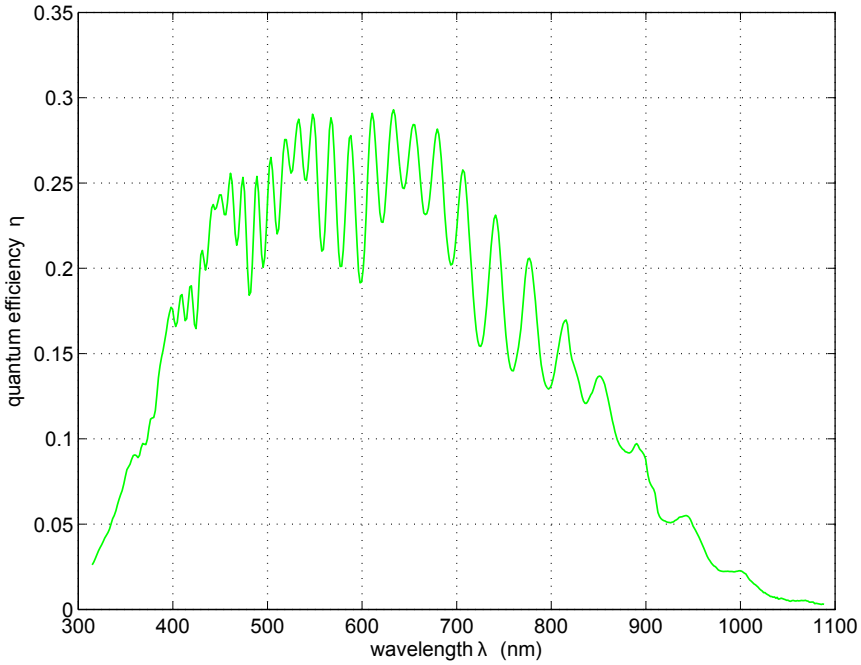


***Figure 15:*** *Example for a spectroscopic measurement of the quantum efficiency in a range from 300–1100 nm with a FWHM of 10 nm, no smoothing is applied.*

The evaluation procedure contains the following steps for every chosen wavelength:

1. Compute the mean spectral gray value.
2. Subtract the mean dark value from the mean spectral values.
3. Divide by $K$, as determined from the linearity and sensitivity measurements (Section 6.6), performed at the *same* operation point, to compute the number of accumulated charge units.
4. Divide by the mean number of photons, $\mu_p(\lambda)$, calculated using the spectral calibration curve Section 9.3 to obtain the quantum efficiency:

$$\eta(\lambda) = \frac{\mu_y(\lambda) - \mu_y.\text{dark}}{K\,\mu_p(\lambda)}. \tag{61}$$

An example curve is shown in Fig. 15.

# 10 Publishing the Results

This section describes the basic information which must be published for each camera and precedes the EMVA 1288 data.

## 10.1 Basic Information

| Item | Description |
|---|---|
| Vendor | Name |
| Model | Name |
| Type of data presented[1] | Single; typical; guaranteed; guaranteed over life time |
| Sensor type | CCD, CMOS, CID, ... |
| Sensor diagonal | in [mm] (Sensor length in the case of line sensors) |
| Lens category | Indication of lens category required [inch] |
| Resolution | Resolution of the sensor's active area: width x height in [pixels] |
| Pixel size | width x height in [$\mu$m] |
| CCD only | |
| Readout type | progressive scan or interlaced |
| Transfer type | interline transfer, frame transfer, full frame transfer, frame interline transfer |
| CMOS only | |
| Shutter type | Global: all pixels start exposing and stop exposing at the same time. Rolling: exposure starts line by line with a slight delay between line starts; the exposure time for each line is the same. Other: defined in the data-sheet. |
| Overlap capabilities | Overlapping: readout of frame n and exposure of frame n+1 can happen at the same time. Non-overlapping: readout of frame n and exposure of frame n+1 can only happen sequentially. Other: defined in the data-sheet. |
| Maximum readout rate | at the given operation point (no change of settings permitted) |
| Dark current compensation | Specify whether camera has dark current compensation |
| Interface type | Analog[2], USB2, IEEE 1394a or b, CameraLink, ... |
| Operation point(s) | Describe operation points used for EMVA 1288 measurements (including gain, offset, maximum exposure time, mode of camera, ...) |
| EMVA 1288 | Specify which test equipment, which release of the EMVA 1288 standard was used and which optional EMVA 1288 data have been measured |

[1] Specify definition used for typical data, e. g., number of samples, sample selection. The type of data may vary for different parameters, e. g., guaranteed specification for most of the parameters and typical data for some measurements not easily done in production. It then has to be clearly indicated which data is of what nature.

[2] Specify frame grabber used with analog camera

## 10.2 The EMVA 1288 Datasheet

The data sheet is structured in the following way:

**Optional cover page** Free for anything. Typical first page from companies (key features, description, picture, etc). Any layout is possible. If present, the first page must contain the EMVA1288 logo.

**General** One or more pages describing the test equipment used, the version of the EMVA 1288 standard used, the basic camera parameters and a summary of the operation points for which measurements are provided (see first page of attached document). If spectrometric measurements are performed, a graph with the wavelength dependency of the

***Table 2:*** *List of all EMVA 1288 parameters with classification into mandatory and optional.*

| Type of measurement | Mandatory | Reference |
|---|---|---|
| Quantum efficiency $\eta$ | Y | Specify center and FWHM wavelengths of the light source used |
| Gain $K$, $1/K$ | Y | units DN/e$^-$ and e$^-$/DN |
| Dark noise | Y | in units DN and e$^-$ |
| $\text{DSNU}_{1288}$ | Y | in units DN and e$^-$ |
| Signal to noise ratio $\text{SNR}_{\max}$ | Y | as ratio and in units dB and bits |
| $\text{SNR}_{\max}^{-1}$ | Y | in % |
| $\text{PRNU}_{1288}$ | Y | in % |
| Non-linearity error $\text{LE}_{\min}$, $\text{LE}_{\max}$ | Y | % |
| Absolute sensitivity threshold | Y | in number of electrons, photons, photons per $\mu\text{m}^2$, specify center wavelength |
| Saturation capacity | Y | in number of electrons, photons, photons per $\mu\text{m}^2$, specify center wavelength |
| Dynamic range (DR) | Y | as ratio and in units dB and bits |
| Dark current | Y | in units DN/s and e$^-$/s |
| Doubling temperature $T_d$ (K) | N | see Section 7.2 |

quantum efficiency (Fig. 15) is included. The date when the measurement was performed must be provided on request.

**Summary page for each operating point** Each page is a summary of the results for one of $N$ operating points (see second page of attached document). The summary page contains a description of the operating point, a graph with the photon transfer curve (Fig. 6), a graph with the SNR curve (Fig. 7) and a one-column table with all quantities according to Table 2, which are detailed in Sections 6–9. Quantities that are not mandatory according to Table 2 must be listed as well to make clear what has *not* been measured. The header contains the EMVA 1288 logo on the left and the company logo on the right.

**Detailed results for each operating point** For each operating point, a set of pages containing the details, large size plots, for each plot a table with the extracted data, for each operating points more specific details about the test conditions (gain, settings, ROI, exposure range, temperature, etc).

A template data sheet is published together with release 3.1 in a separate document, which has been generated by the EMVA 1288 reference implementation (`https://github.com/emva1288`). It clearly specifies which graphs and camera parameter must be placed where in the data sheet. It also details all the axes labeling of the graphs.

# A Bibliography

[1] Aster, R. C., Borchers, B., and Thurber, C. H.: Parameter Estimation and Inverse Problems, vol. 90 of *International Geophysics Series*, Academic Press, Boston, 2 edn., doi: 10.1016/B978-0-12-385048-5.00030-6, URL https://sites.warnercnr.colostate.edu/aster/2014/07/24/parameter-estimation-and-inverse-problems/, 2013.

[2] Denvir, D. J. and Conroy, E.: Electron multiplying CCDs, in: Optical Metrology, Imaging, and Machine Vision, edited by Shearer, A., Murtagh, F. D., Mahon, J., and Whelan, P. F., vol. 4877 of *SPIE Proc.*, pp. 55–68, 2003.

[3] DeWeert, M. J., Cole, J. B., Sparks, A. W., and Acker, A.: Photon transfer methods and results for electron multiplication CCDs, in: Applications of Digital Image Processing XXVII, edited by Tescher, A. G., vol. 5558 of *SPIE Proc.*, pp. 248–259, 2004.

[4] Dierks, F.: Sensitivity and Image Quality of Digital Cameras, Tech. rep., Basler AG, 2004.

[5] Holst, G. C. and Lomheim, T. S.: CMOS/CCD Sensors and Camera Systems, SPIE Press, Bellingham, Washington, USA, 2 edn., 2011.

[6] Janesick, J., Klaasen, K., and Elliott, T.: CCD charge collection efficiency and the photon transfer technique, in: Solid State Imaging Arrays, edited by Dereniak, E. L. and Prettyjohns, K. N., vol. 570, pp. 7–19, Proc. SPIE, doi: 10.1117/12.950297, 1985.

[7] Janesick, J. R.: Scientific Charge-Coupled Devices, SPIE, Bellingham, WA, doi: 10.1117/3.374903, 2001.

[8] Janesick, J. R.: Photon Transfer, SPIE Press, doi: 10.1117/3.725073, 2007.

[9] Jähne, B.: Digital Image Processing, Springer, Berlin, 6 edn., doi: 10.1007/3-540-27563-0, 2005.

[10] Labsphere: A Guide to Integrating Sphere Theory and Applications, technical guide, see http://www.labsphere.com/, 2003.

[11] Labsphere: Integrating Sphere Uniform Light Source Applications, technical guide, see http://www.labsphere.com/, 2003.

[12] Montgomery, D. C., Peck, E. A., and Vining, G. G.: Introduction to Linear Regression Analysis, John Wiley & Sons, 5 edn., URL http://eu.wiley.com/WileyCDA/WileyTitle/productCd-0470542810.html, 2012.

[13] Theuwissen, A. J. P.: Solid-State Imaging with Charge-Coupled Devices, Kluwer Academic Publishers, doi: 10.1007/0-306-47119-1, 1995.

[14] Widrow, B. and Kollar, I.: Quantization Noise — Roundoff Error in Digital Computation, Signal Processing, Control, and Communications, Cambridge Univ Press, URL www.cambridge.org/9780521886710, 2008.

# B Notation

This section summarizes the used notation in two tables. The first table describes all quantities used, the second table, the meaning of indices that are used with various quantities. With this split in the description, the notation tables are much shorter.

| Quantity | Units | Description |
|---|---|---|
| $A$ | $\mu m^2$ | Area of a sensor element (pixel) |
| $c$ | m/s | Velocity of light |
| $d$ | mm | Distance of sensor plane to opening (aperture) of light source |
| $D$ | mm | Diameter of opening (aperture) of light source |
| $D'$ | mm | Diameter of image sensor |
| $DSNU_{1288}$ | DN | Dark signal nonuniformity |
| DR | 1, dB, bits | Dynamic range |
| $E$ | $W/m^2$, Photons/(s pixel) | Irradiance at sensor plane |
| $h$ | Js | Planck constant |
| $H$ | $Ws/m^2$, Photons/pixel | Irradiation (exposure) at sensor plane |
| $k$ | $m^{-1}$ | wave number |
| $K$ | $DN/e^-$ | Overall system gain of a digital camera |
| $PRNU_{1288}$ | % | Photo response nonuniformity |
| SNR | 1, dB, bits | Signal to noise ratio |
| $\boldsymbol{p}$ | — | Power spectrum |
| $R$ | DN/p | Responsivity (slope characteristic curve) |
| $s$ | — | *spatial* standard deviation of the quantity put into the index |
| $s^2$ | — | *spatial* variance of the quantity put into the index |
| $\boldsymbol{s}$ | DN | Digital image sequence |
| $t_{exp}$ | s | Exposure time |
| $y$ | DN | Digital gray value |
| $\boldsymbol{y}$ | DN | 2-D digital image |
| $\eta$ | 1 | Total quantum efficiency, def. Eq. (1) |
| $\lambda$ | nm | wavelength of light |
| $\mu$ | — | mean of the quantity put into the index |
| $\nu$ | Hz | frequency of light |
| $\sigma$ | — | *temporal* standard deviation of the quantity put into the index |
| $\sigma^2$ | — | *temporal* variance of the quantity put into the index |

| Index | Units | Description |
|---|---|---|
| d | $e^-$ | relates to dark signal in units of $e^-$ |
| dark | DN | relates to dark signal in units of DN |
| e | — | relates to number of electrons |
| min | — | relates to absolute sensitivity threshold |
| p | — | relates to number of photons |
| q | — | relates to quantization noise |
| sat | — | relates to saturation of the sensor |
| [l] | — | selection of an image in a image sequence, $l$ runs from 0 to $L-1$ |
| [m] | — | selection of a row in a image, $m$ runs from 0 to $M-1$ |
| [n] | — | selection of a column in a image, $n$ runs from 0 to $N-1$ |

# C Changes to Release A2.01

This section summarizes the changes of release 3.0 over the previous release A2.01 of the EMVA 1288 standard. Mostly, only extensions were added to the standard as described in Section C.1. To improve the standard and simplify its usage some minor changes were necessary. All these changes were implemented in release 3.0 in a way so that the data of cameras measured according to the specifications of release A2.01 are still valid.

## C.1 Added Features

The following features are added to release 3.0 of the standard:

1. Color sensors and color cameras and not only gray scale cameras are now covered
2. Flexible characterization of defect pixels via logarithmic histograms (Sections 4.3 and 8)

## C.2 Extension of Methods to Vary Irradiation

In release A2.01 of the standard, the photon transfer method (sensitivity and noise measurements) had to performed with a continuous light source and varying exposure times, while the linearity measurements had to be measured with a constant exposure time and a pulsed light source with varying pulse widths. This was awkward, because the same type of measurements had to be performed twice.

With release 3.0 of the standard, any method described in Section 6.3 can be used to vary the irradiation and so the *same* set of measurements can be used to evaluate the data according to the photon transfer method (Section 6.6) and to determine the linearity error (Section 6).

## C.3 Modifications in Conditions and Procedures

The following measuring conditions have been unified, described more precisely, or been changed:

1. For the photon transfer method, the mean value has to be computed from *both* images according to Eq. (28), and not only from the first as in release A2.01.
2. Condition to set the offset of the camera in order to avoid underflow with linearity measurements and nonuniformity measurements (Section 6.5). In release A2.01 different conditions were prescribed for linearity measurements, photo transfer measurements, and nonuniformity measurements.
3. The number of measuring points for sensitivity, linearity, and noise measurements is increased to 50. Only for production measurements as few as 9 values are allowed.
4. Number of images to be used for nonuniformity measurements. It is now possible to perform these measurements with just 16 images for inline inspection by correcting the bias caused by the residual temporal noise (Section 8).
5. The spatial noise is no longer contained in the definition of the SNR (compare Eq. (11) with Eq. 15 of release A2.01. This change has been made, because it is possible to reduce the spatial nonuniformities by suitable shading correction techniques with a single image, while this is not possible with the temporal noise.
6. The condition for the gray value range for the regression of the mean gray values against the irradiation has been better adapted to possible nonlinearities in this relation. In release A2.01 it was at least the range from the dark image to 80% of the maximum temporal variance (Section 6.6), now it is reduced to 70%.
7. For a computation of the absolute sensitivity threshold the more accurate equation Eq. (17) is used. This change was required because the old equation without the correction term 1/2 in release A2.01 is not accurate enough for cameras with a very low dark noise of only a few electrons.
8. The linearity $LE$ must be specified for the interval of 5–95% of the saturation points (Section 6.7).

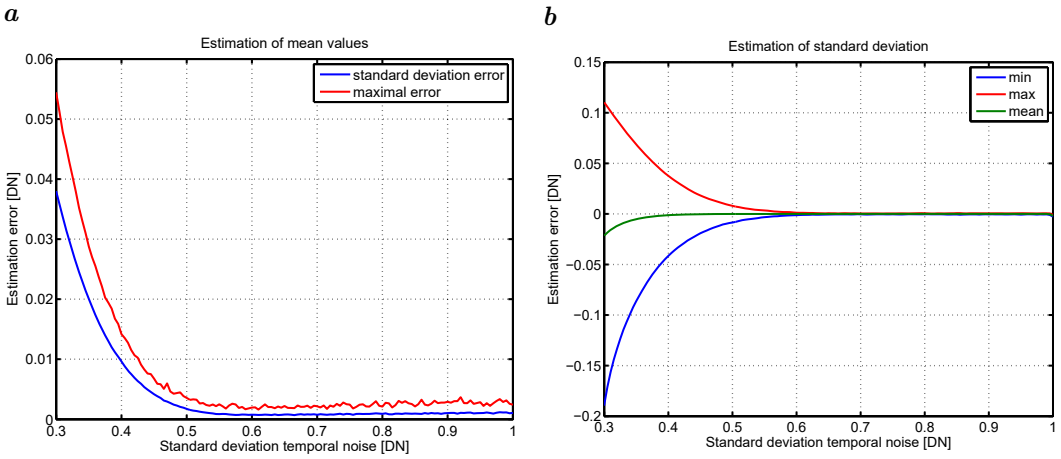


***Figure 16:*** *Results from Monte Carlo simulations for the estimation of* **a** *the mean value and* **b** *the standard deviation of the digital gray value as a function of the standard deviation in units of digital numbers [DN] in the range between 0 and 1.*

9. For dark current measurements a minimum number of six equally spaced exposure times must be used (Section 7.1).
10. For a proper analysis of defect pixels, a highpass filtering is introduced so that the PRNU measurements are not spoiled by the imperfections of the used light source (Section 4.4). This highpass filtering is used also before *all* other nonuniformity evaluations including the estimation of spatial variances (Section 8.1) except for the computation of the spectrograms and all quantities derived from them (Section 8.2).
11. Measuring conditions for spectral measurements are relaxed (Section 9). The $f$-number can now deviate from 8, but must be reported.

### C.4 Limit for Minimal Temporal Standard Deviation; Introduction of Quantization Noise

In the previous releases of the standard, quantization noise was neglected in the linear camera model. This led to a more complicated measuring procedure with low-resolution digitalization, i. e., 8 bit cameras. The problem resulted from the fact that the standard deviation of the temporal noise in the dark image may become smaller than the quantization interval.

Versions 1 and 2 of the EMVA 1288 standard therefore recommended:

*"The gain setting of the camera is as small as possible but large enough to ensure that in darkness*

$$K\sigma_d \geq 1$$

*holds true (Otherwise, the quantization noise will spoil the measurement.)"*

It turns out that this limit is too cautious [14]. Monte-Carlo simulations were performed to check how accurate the mean and the variance can be estimated as a function of standard deviation $\sigma_y$ in units DN. For the simulations 201 mean gray values equally distributed between 0 and 1 were taken and zero-mean normally distributed noise was added to the values. The estimated mean and variances were averaged over 900 000 realizations of each value. Finally, the deviations in the estimations were averaged over all 201 values.

The results are shown in the range $[0.3, 1]$ for $\sigma_y$ in Fig. 16. The mean gray value can be estimated with a maximum error of less than 0.014 DN even for standard deviations as low as 0.4 DN (Fig. 16b). The estimate of the standard deviation is biased by the additional standard deviation of the quantization, $\sigma_q = \sqrt{1/12}$. However, if the estimate of the standard deviation is corrected for the additional effect of the standard deviation of the quantization error (unbiased estimation)

$$\sigma_y^2 = \sigma_{\text{est}}^2 - \sigma_q^2 = \sigma_{\text{est}}^2 - 1/12, \tag{62}$$

the maximum error of the estimate remains below 0.04 even for standard deviations as low as 0.4. The variation in the estimation of the standard deviation comes from the different positions of the mean in the $[0, 1]$ interval. If it is close the edge of the interval, the values flip often either to the higher or lower value, resulting in a higher standard deviation. If the mean is in the middle of the interval this happens less frequently, so that the standard deviation is lower.

In conclusion, the variance $\sigma^2_{y.\mathrm{dark}}$ must be larger than $0.24\,\mathrm{DN}^2$. Subtracting the quantization noise variance $\sigma^2_q = 1/12\,\mathrm{DN}^2$, this results in a minimal detectable temporal standard deviation of 0.40 DN. If the measured temporal variance is smaller than $0.24\,\mathrm{DN}^2$, two things can be stated:

1. The dynamic range is limited by the quantization noise (and the maximum possible but not determinable temporal noise to $\mu_{y.\mathrm{sat}}/0.49$.
2. The standard deviation of the dark noise in units $\mathrm{e}^-$ can be estimated to $\sigma_d < 0.40/K$.

The correction of the temporal noise by the quantization noise, which is possible down to a measured temporal noise variance of 0.24, expands the measurable dynamic range of a camera by a factor of about 2 over the condition of release A2.01. For a 8-bit camera, the maximum and measurable dynamic range is $255/0.49 \approx 500$

### C.5 Highpass Filtering with Nonuniformity Measurements

The highpass filtering with defect pixel measurements is implemented by subtracting a $5 \times 5$ box-filtered image from the original mean images:

$$\boldsymbol{y}' = \boldsymbol{y} - {}^5\boldsymbol{R} * \boldsymbol{y} \quad \text{with} \quad {}^5R = \begin{bmatrix} 1 & 1 & 1 & 1 & 1 \\ 1 & 1 & 1 & 1 & 1 \\ 1 & 1 & 1 & 1 & 1 \\ 1 & 1 & 1 & 1 & 1 \\ 1 & 1 & 1 & 1 & 1 \end{bmatrix} /25. \tag{63}$$

The transfer function of this highpass filter is given by [9, p. 303]:

$${}^p\hat{h}(\tilde{k}_1, \tilde{k}_2) = 1 - \frac{\sin(\pi P \tilde{k}_1/2)}{P \sin(\pi \tilde{k}_1/2)} \cdot \frac{\sin(\pi P \tilde{k}_2/2)}{P \sin(\pi \tilde{k}_2/2)}, \tag{64}$$

where $P = 5$ and $\tilde{k}_1$ and $\tilde{k}_2$ are the wave numbers in horizontal and vertical direction, respectively, normalized by the spatial Nyquist frequency. This type of highpass filtering removes only a small fraction of the white noise. This can be computed by integrating over the squared transfer function

$$s^2_{y'} = s^2_y \int_{\tilde{k}_1=0}^{1} \int_{\tilde{k}_2=0}^{1} \hat{r}^2(\tilde{k}_1, \tilde{k}_2)\, \mathrm{d}\tilde{k}_1 \mathrm{d}\tilde{k}_2 = s^2_y (1 - r_{0,0})^2 = s^2_y \left(1 - \frac{1}{P^2}\right)^2 = 0.92\, s^2_y, \tag{65}$$

provided that the spectrum of the random spatial variations is white (Section 4.2). Thus this method efficiently suppresses low-frequency spatial variations of the light source without reducing the estimate of the variance of the white noise significantly. For the proposed $5 \times 5$ box filter ($P = 5$), the reduction in the standard deviation is just 4%: $\sigma_{y'} = 0.96\,\sigma_y$. Therefore the measured spatial standard deviation $s_{y'}$ must be divided by 0.96 in order to obtain the correct value $s_y$.

For all further processing leave out two border lines at the top and bottom and two border columns on the left and right of the filtered image, because the filtering will not be exact in these areas. This procedure reduces the image size by four lines and four rows.

For line-scan cameras only a horizontal $5 \times 1$ box filter is applied. Therefore the correction factor is in this case (compare Eq. (65))

$$s^2_{y'} = s^2_y \int_{\tilde{k}_1=0}^{1} \hat{r}^2(\tilde{k}_1)\, \mathrm{d}\tilde{k}_1 = s^2_y (1 - r_0)^2 = s^2_y \left(1 - \frac{1}{P}\right)^2 = 0.64\, s^2_y. \tag{66}$$

The measured spatial standard deviation for line cameras $s_{y'}$ must be divided by 0.80 in order to obtain the correct value $s_y$. For all further processing of highpassed average nonuniformity images from line cameras leave out two border columns on the left and right.

# D Changes to Release 3.0

This section summarizes the changes of release 3.1 over release 3.0 of the EMVA 1288 standard.

## D.1 Changes

The changes include:

1. Spectral specification of light source (Section 6.2): Light source must also be specified by controid wavelength $\lambda_c$. This wavelength should also be used instead of the peak wavelength $\lambda_p$ for computation of the number of photons according to Eq. (2).
2. In some cases, just taking the maximum value of the variance in the photon transfer curve does not lead to a correct estimate of the saturation gray value (Section 6.6). Therefore the simple maximum search is replaced by a more sophisticated algorithm.
3. Changed algorithm to compute non-linearity: relative deviations are used instead of absolute deviation in order to account for the higher dynamic range of modern image sensors (Section 6.7).
4. The non-whiteness factor for the spatial variance of DSNU and PRNU (Section 8.2) is no longer reported, because the algorithms used in release 3.0 proved to be not reproducible enough to be a useful figure. If improved algorithms will be found in the future, the quantity will be incorporated again in an upcoming release.
5. Changed algorithm to compute bin width of logarithmic histograms for improving appearance of graphs without gaps (Section 8.4).

## D.2 Added Features

The following features are added to release 3.1 of the standard:

1. Most importantly, release 3.1 now includes a template data sheet (Section 10.2)
2. Addition of total SNR: Definition is in Section 8.1, model curve according to Eq. (48) is added to SNR plot in Fig. 7.
3. Plots of horizontal and vertical profiles (Section 8.3).

# E List of Contributors

EMVA gratefully acknowledges the active contributions to release 3.1 of this standard by the following members of the EMVA 1288 standardization committee, given in alphabetic order:

- Aphesa SPRL, Harzé, Belgium
- Basler AG, Ahrensburg, Germany
- e2v technologies plc, Essex, England
- HCI, Heidelberg University, Heidelberg, Germany
- Image Engineering GmbH & Co. KG, Köln, Germany
- JAI A/S, Copenhagen, Denmark
- MATRIX VISION GmbH, Oppenweiler, Germany
- Matrox Electronic Systems Ltd., Dorval, Quebec, Canada
- PCO AG, Kelheim, Germany
- STEMMER IMAGING GmbH, Puchheim, Germany
- SVS-VISTEK GmbH, Seefeld, Germany
- TVI Vision Oy, Helsinki, Finland

The history of the EMVA 1288 dates back to 2004. Among the initiators were Martin Wäny (Awaiba) and Fritz Dierks (Basler AG). Other major initial contributions came from Albert Theuwissen (Dalsa) and Emil Ott (PCO AG). Release A01 was issued in August 2005, Release A02 in August 2007 and Release 3 in November 2010. The founding chair was Martin Wäny. Since 2008 the EMVA 1288 committee is chaired by Bernd Jähne (HCI, Heidelberg University).